Reference Stratigraphy
Applied to Rock Mechanics Studies
for the Waste Isolation Pilot Plant:
A Review - January 11, 2017

Dennis W. Powers, Ph.D.
Consulting Geologist

Summary

Reference stratigraphy for the Waste Isolation Pilot Plant (WIPP) was developed to provide a standard for comparing the results of different models of mechanical behavior of the WIPP underground (e.g., Krieg, 1984) (Figure 1). Munson et al. (1989) revised the reference stratigraphy (Figure 2), and they concluded that mechanical behavior at WIPP was better represented by a different distribution of lithologies, in particular by assigning most of the units in the reference stratigraphy to "argillaceous halite" rather than as "clean halite." Here I re-evaluate the background for these reference stratigraphies and lithology by examining core and other data.

Some archived cores held by Sandia National Laboratories (SNL) in reserve for rock mechanic studies have been surveyed visually for lithologic features and, more specifically, non-halite proportions and distribution. Seven large diameter (30.48 cm; 12 inch) core segments were uncrated and visually examined; three cores are considered "clean" halite, and four cores are "argillaceous" halite. These cores were taken from the WIPP by horizontal drilling in the northern part of the facility.

The cores from "clean" halite intervals consist of mainly light orange halite up to ~3 cm (~1 inch) diameter, lesser gray halite, and local very coarse (up to 10 cm; 4 inches) clear halite. There is little to no discernible clay in the orange halite, and sulfate is estimated to be less than 0.5% by volume. Gray halite locally includes up to 2-3% sulfate, by volume, with minor clay. Non-halite minerals are unevenly distributed and are principally intercrystalline blebs and films. Core segments SNLCH105-3&4 display crudely stratified orange and gray halite. Core segment SNLCH106-8 reveals very large clear halite crystals I interpret as cements that filled syndepositional dissolution pipes. These features are consistent with the cored location in mapping unit 3 (MU-3) (see Figure 9).

Cores from "argillaceous" halite consist of zones or intervals of a) relatively fine (<~5 mm; 0.2 inch) light brown or slightly orange halite and b) coarser (up to 2.5 cm; 1 inch) halite that is more translucent and lighter in color than the fine halite. Overall, the non-halite components in the "argillaceous" halite appear to average ~1% but are higher in coarser halite. The clay proportion dominates in the coarser halite intervals, and sulfate dominates the fine halite intervals. Clay is not uniformly distributed. Some occurs as distinctive irregular blebs between crystals, but clay also forms thin (e.g. 2-3 mm; 0.08-0.12 inch), irregular, curved, discontinuous stringers. The features and halite fabrics are generally consistent with MU-0, where the

cores were taken. The features developed on a salt pan that is subaerially exposed much of the time, producing efflorescent salt (fine halite) in "podular" features, as well as saucers and mudcracks (coarser halite with clay stringers). Syndepositional dissolution pipes cemented by coarse halite are also common in MU-0.

The gross non-halite fraction is estimated (visually) as 1% or less. The "clean" halite tends to include mainly sulfate while the "argillaceous" halite usually includes more clay than sulfate.

I also examined two vertical cores, each ~15 m (50 ft) long, that were taken up and down from the SDI area underground (Figure 3). The cored location is ~150 m (500 ft) from Room D; the cores are the closest known available for assessing argillaceous halite within the reference stratigraphy in this area.

The down core is consistent with stratigraphy and lithology reported early from WIPP (e.g., Krieg, 1984). There are no true argillaceous halites (by visual estimate), and individual clays (e.g., base of anhydrites) are recognized.

The up core is also consistent with reported descriptions of MUs. Much of the halite is very low in clay content. Three argillaceous halites and several individual clays known from previous work are present. The upper part of H-7 is relatively argillaceous and transitions into one of the argillaceous halites.

From a geological perspective, argillaceous halite is not the principal lithology in the reference stratigraphy.

Two areas stand out in this review: scale and lack of analyses of clay (and other possible factors) that correspond directly to samples tested for mechanical properties. Scale enters because most identifiable MUs can vary locally in crystal size, fabric, and non-halite content. The depositional environment of most argillaceous halite beds creates scale problems for consistency between small (cm-dm scale) samples. Few samples have been identified for which the various factors have been

detailed. Although weight percent insolubles can be quantified after mechanical testing, fabrics, crystal size, distribution of non-halite components, and other possible factors may have to be carefully characterized prior to mechanical testing.

The cores that I examined and reported on here regarding reference stratigraphy at WIPP are representative of strata that are distinct in minor and trace minerals and their distribution. These two strata also display differences in halite textures. The two strata are readily differentiated in clean "outcrop" underground and in good cores. Nevertheless, as I pointed out in the descriptions and discussion of these cores, variability within units at the cm-dm scale, especially in the lower unit, can result in samples from within a unit that differ considerably by minor and trace mineral content and distribution as well as halite fabrics. In addition, some subsamples from different units may be visually indistinguishable because of features such as dissolution pipes that may cut both units or present similar fabrics and trace mineral contents.

With this in mind, I have recommended that subsamples be individually described for these visual properties prior to mechanical testing and be subjected to thorough determination of the minor and trace minerals through destructive testing after mechanical testing is complete.

In view of these conditions, it is not possible for me to assert that the subsamples taken for mechanical testing all represent argillaceous halite or clean halite as we understand them at the macro level for these sampled intervals.

Introduction

Frank Hansen (SNL) asked me to re-evaluate the reference stratigraphy and lithologic assignments for the interval commonly used in rock mechanics modeling for the WIPP.

Information Only

One of the steps in the re-evaluation is to examine lithology with respect to large diameter (30.48 cm; 12 inch) cores drilled horizontally in the northern end of the WIPP underground (Figure 3). Some of these cores have been used for laboratory investigations of mechanical properties of the horizons, and the coring levels were selected to represent differing lithologies: "argillaceous" halite and "clean" halite. In initial sections, I report the results of the partial examination of some of the remaining large-diameter cores retained by SNL.

Another step in the re-evaluation was to examine smaller diameter cores taken up and down ~15 m (50 ft) from excavations in the vicinity of the SDI underground at WIPP (Figure 3). These cores are the most recent known taken in an area relatively close to Room D (and other experimental areas) where it has been suggested (Munson et al., 1989) that the dominant lithology through the reference stratigraphy is argillaceous halite. The results of the SDI core re-examination follow description and discussion of the large-diameter cores taken by SNL.

Prior to re-examining cores, I also examined some of the literature regarding the development of the reference stratigraphy. I discuss some of the development of the reference stratigraphy, tied to work on the Salado, and relate this in part to the work in rock mechanics as well as geology.

Background to Halite Distinctions

Stratigraphy and Lithology

Early reports of geology from WIPP distinguish between halite beds in the Salado. Jones (1981) included the lithologic descriptions of core from ERDA-9, the initial test in 1976 of the geology near the center of the WIPP site. Jones (1981) described some intervals I associate approximately with the underground exposures and mapping units as follows:

"Halite, light-gray, medium-crystalline, argillaceous and sparingly polyhalitic" (MU-4; 2163.7-2164.7 ft depth),

"Halite, light-yellow, medium-to coarse-crystalline, sparingly polyhalitic" (MU-3; 2166.9-2164.7 ft depth),

"Halite, light-greenish-gray, fine-to medium-crystalline, argillaceous" (MU-2; 2167.4-2166.9 ft depth),

"Halite, light-brown, fine- to medium-crystalline, very sparingly argillaceous throughout and sparingly polyhalitic" (MU-1+; 2170.5-2167.4 ft depth). [I attribute the extra depth to this unit as core through probable dissolution pipes (further noted later).]

Jones (1978) described the basic lithology from cuttings and cores of the Salado Formation that were taken in 1976 for determining the extent of potash deposits at WIPP. Although the descriptive text varies somewhat for the 21 boreholes in that survey, beds of halite were described in terms indicating vertical variation, including intervals of very low or no clay content.

Underground access through the shafts from late 1982 on provided additional detail, and visible lateral continuity of distinctive units led to the designation of mapping units (e.g., TSC-D'Appolonia, 1983). Unit 3 (later commonly called MU-3) is described as "Halite: colorless to moderate-reddish-orange; transparent to translucent; coarsely crystalline; trace of dispersed polyhlaite; polyhalite content commonly decreases upward . . .". Unit 0 (MU-0) is described as "Argillaceous halite . . .".

Detailed shaft mapping by Holt and Powers (1984, 1986, 1990) provided similar evidence of vertical variation in the clay and sulfate content of the Salado halite beds, attributing the vertical variations and detailed features to a general desiccating-upwards cycle of deposition (Holt and Powers, 1990, 2011).
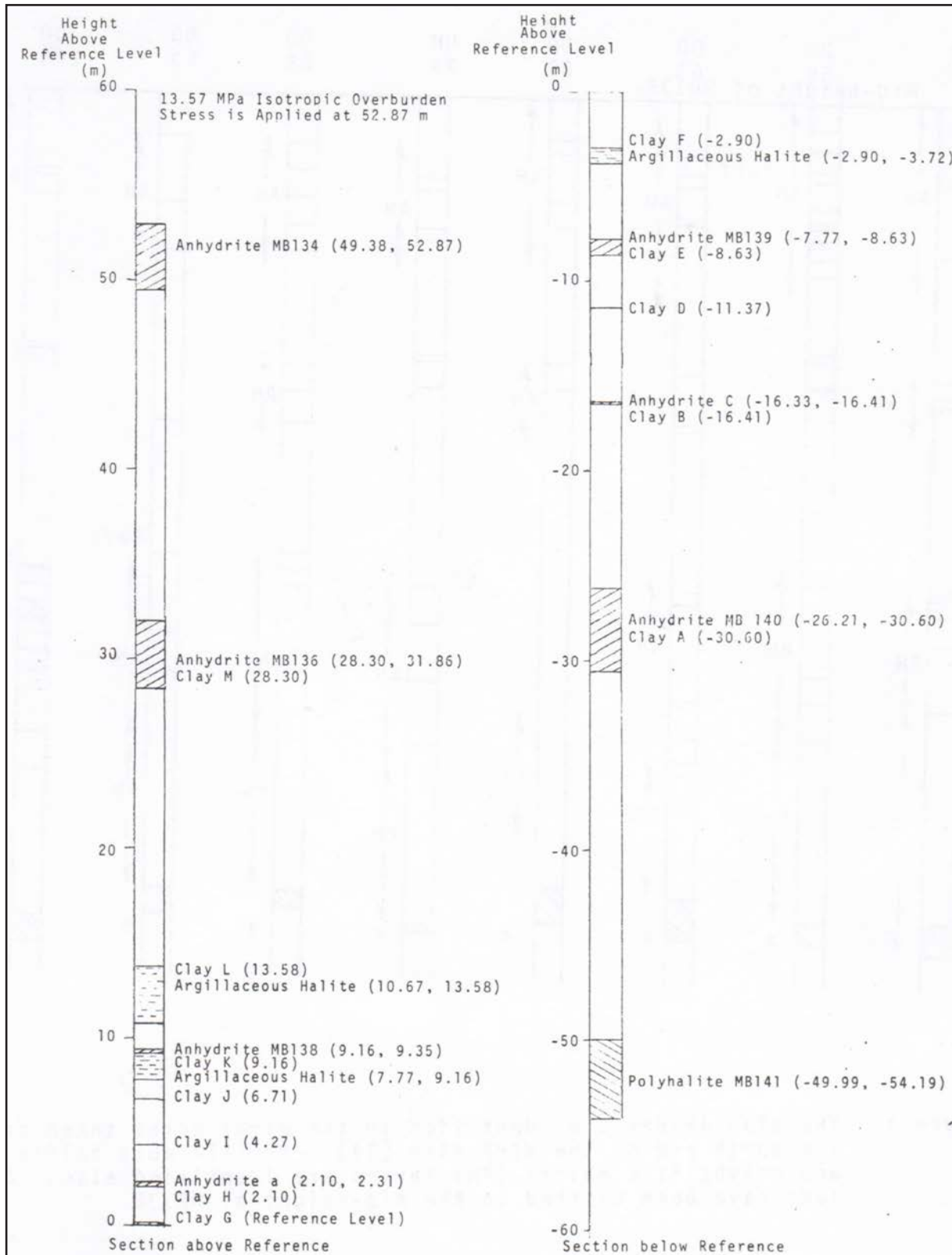
Figure 1. September 1983 reference stratigraphy. From Krieg (1984, p. 32). Original figure caption notes that anhydrite b should not be used in a structural model and was included for reference purposes. It is not shown in the figure but lies immediately above Clay G.
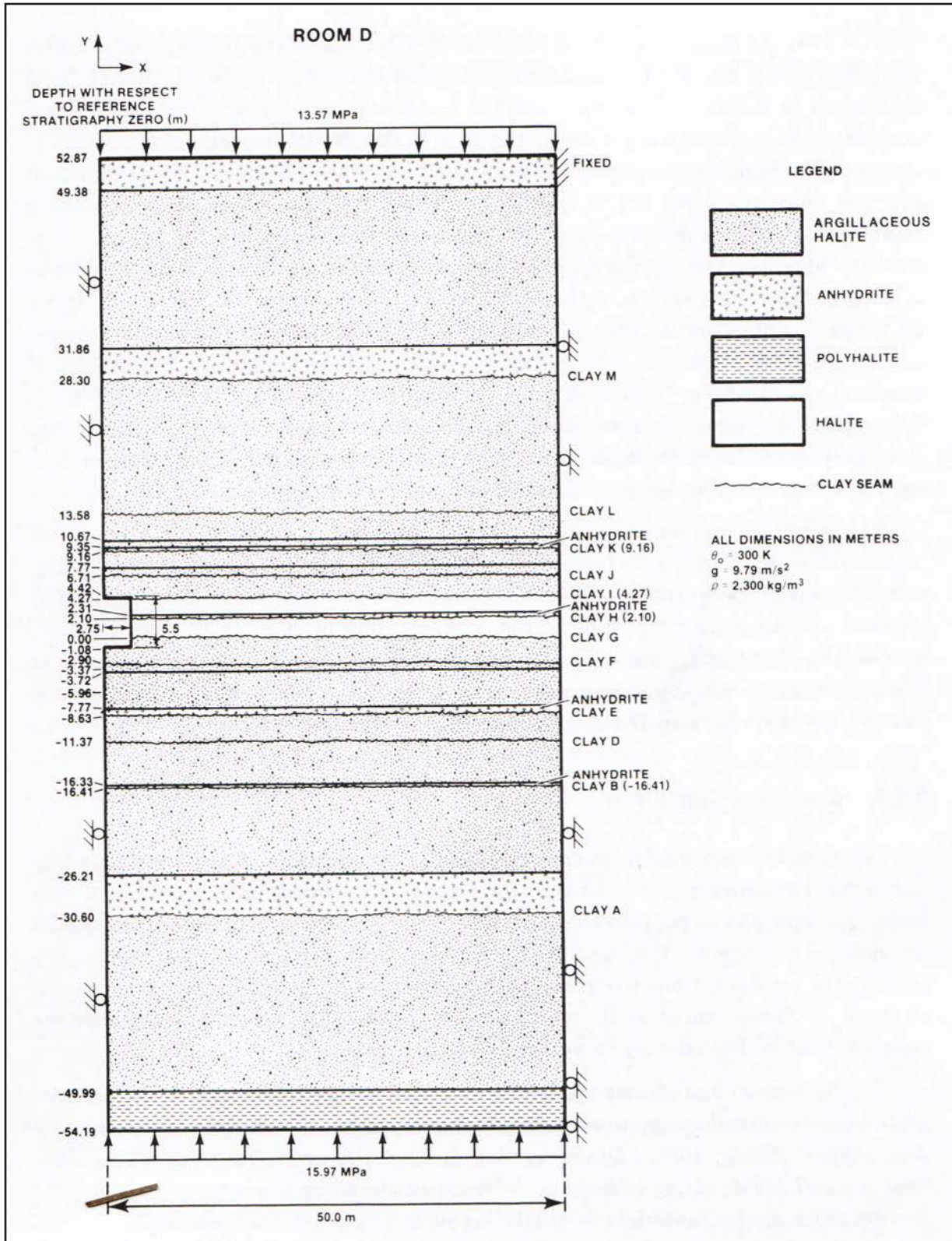
Information Only

Figure 2. Reference stratigraphy from Munson et al. (1989, p. 47, figure 3-3).

Information Only

Separate from WIPP studies, Lowenstein (1988) described depositional cycles for the Salado, utilizing terms such as halite-rich and mud-rich to distinguish halitic intervals.

Salado halite beds at the WIPP site have been known to vary lithologically since early investigations. These variations were incorporated into Krieg (1984) (Figure 1) and other early versions of the reference stratigraphy for rock mechanics modeling. Later, Munson et al. (1989) (Figure 2) asserted that halite within the reference stratigraphy was mainly represented by "argillaceous" halite with only limited "clean" halite in an interval above the initial disposal horizon. This assertion is addressed here, as I have examined recent cores and descriptions of some previous cores through the reference stratigraphy interval.

Non-Halite Fraction of Halite Beds

Descriptors and estimates of clay content of Salado halite have been quite variable in the earlier history of WIPP work. Visual estimates notably overestimated clay content. Early work by Bodine (1978) provided a broad perspective on clay mineralogy and proportions. Details of the work not provided in Bodine (1978) were included in Powers et al. (1978) in Chapter 7. It is clear from the limited statistics available there that EDTA-insoluble content in "rock salt" beds was rarely above 1 weight percent and was <0.1 weight percent for some "rock salt" samples. Mineralogical analysis showed a variety of silicates, including clays, quartz, and feldspar.

Stein (1983) presented data on mineral residues from 28 samples from 2 cores inferred to be 15 m (50 ft) long, one up and one down and likely approximating the reference stratigraphy. The coreholes are apparently designated DO-52 and DO-53; no location is indicated. [US DOE (1985) reports (Table 10-3) that both boreholes are located at N146, W4. Depths to units are such that DO-52 is an up hole and DO-53 is a down hole.] All analyzed samples are surely of halite beds, as the weight percent of water insoluble material ranges from 0.01-5.27. Weight percent EDTA-insoluble[1] material relative to bulk rock is not directly calculated, although weight percent EDTA-insolubles is calculated for the water-insoluble residue. Inspection shows EDTA-insoluble percentages (of the water-insoluble fraction) from reliable samples ranging from 89.28% to 33.60%. Maximum acid-insoluble residue weight percent for a whole sample is ~4%. Stratigraphy and lithology are not presented in this memorandum.

Stein (1985) analyzed 43 samples from two cores, each ~15 m (50 ft) long, taken from the back and floor at Test Room 4. Visual inspection of the results indicates reasonable correspondence of higher EDTA-insoluble percentages for those zones identified as argillaceous. EDTA-insoluble residues ranged from 0.001-5.68 weight percent. Seven samples exceeded 1.0 weight percent. Thirteen samples were 0.01 weight percent or less.

An important aspect is that Stein (1985) indicates these samples were taken to correspond to samples for rock mechanics testing by W. Wawersik (SNL). I have not tracked down the rock mechanics tests to determine what relationship, if any, was found to the results of Stein's analyses.

Senseny (1986) reported that triaxial compression creep tests on argillaceous and clean salt from WIPP showed that the "… small quantity of impurities corresponded to consistent, but small, increases in the deformation measured during the tests." The single clean salt sample included 0.09 weight percent water insolubles and 0.02 weight percent EDTA insolubles. Senseny reports 1.44 ± 1.16 weight percent mean water insolubles in

---

[1] Bodine and Fernalld (1973) popularized the use of EDTA to remove sulfate and carbonate minerals as constituents in argillaceous rocks with minimal alterations of clay minerals.
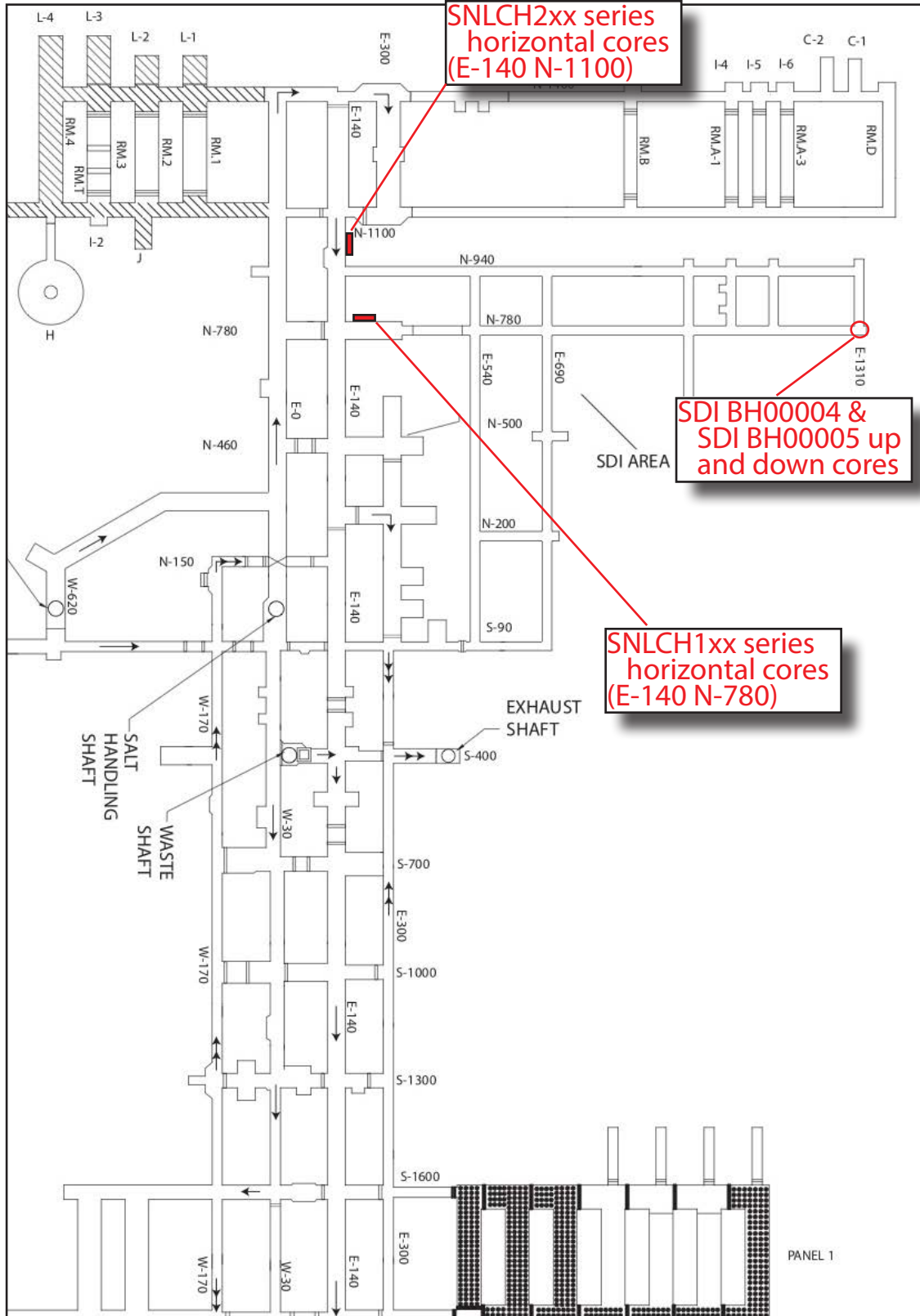
Figure 3. Approximate locations of SNLCH-XXX horizontal cores described in this report. Vertical (up and down) coreholes in SDI are nearest Room D and are discussed here and in Appendix B.

argillaceous halite samples; EDTA-insolubles average 0.72 ± 0.59 weight percent. The mean weight percent of EDTA-insolubles of the water-insoluble portion in the argillaceous amples is 52.6 ± 13.38. [Note: data in Table 2-1 of Senseny differ slightly in the averages and standard deviation when recalculated, most likely due to additional significant figures used for the original calculations. These differences are small.]

Senseny (1986) refers to tests of Permian San Andres salt from the Palo Duro basin (Hansen et al., 1985). An online report (Hansen et al, 1987) is likely the same report. Hansen et al., 1987) classed samples by differing impurity content. In general, these samples contain higher non-halite content (~5-25%) when compared to Salado halites in the Senseny (1986) report. Hansen et al. (1987) report that anhydrite and halite do affect creep, with anhydrite the stronger influence. "No correlation exists between the amount of clay and the creep response. Variability of test results is not readily explained by amount and type of impurities." (Hansen et al., 1987, p. iii).

Hansen et al. (1987, p. 6) also show that the nominal (visual) assignments of rocks to classes defined by amount and type of non-halite constituents "… are not substantiated" by various laboratory evaluations. This was true at WIPP during early underground mapping, and more recent visual estimates, informed by laboratory results, may be better overall. Fabric and distribution of impurities in salt may be important, as well as the total content, and I don't believe those factors are included in most analyses.

Mellegard and Pfeifle (1993) provide creep data on samples assigned to clean and argillaceous halite; there are no data known to me regarding the clay content of these samples.

Krumhansl et al. (1990) sampled two argillaceous units ("clay f" and mapping unit 1 just below the orange marker bed) over drifts from S-N and to the west. The 75 samples

were examined intensively for mineralogy and geochemical properties. Although they presented relative proportions of different clay types for the units, there is no attached data about the weight percent of EDTA-insoluble (silicate) minerals. They note different minerals are present, including quartz.

SNL Core Examination

Two series of large-diameter (30.48 cm; 12 inch) cores were obtained from the WIPP underground by SNL for rock mechanics tests. Some of these cores have been used in laboratory experiments in Germany. The series with designators SNLCH-10x-x have been obtained from MU-3, which is generally considered to be "clean" halite that includes polyhalite but little clay. The series with designators SNLCH-20x-x all have been collected from MU-0. I was able to confirm the stratigraphic locations of these core series during an underground exam of other cores in April 2016 (Figure 3).

The observations reported here for these cores are somewhat generalized rather than trying to describe a separate set of features and textures for each core segment. In a later section, I will discuss how these features and textures fit into the depositional cycle and what that means for heterogeneity of samples.

"Clean" Halite Cores

Three core segments from this lithotype were examined: SNLCH105-3&4, SNLCH106-6 and SNLCH106-8.

These cores are dominated by orange halite that is coarse (generally ~1-3 cm; 0.4-1+ inch) and includes blebs of polyhalite and visible 1-4 mm (0.04-0.16 inch) empty fluid inclusions on the core surface. Polyhalite content is visually estimated < 0.5% volume overall; local zones exceed 1%. Clay was not discernible in the coarse orange halite from these cores. Gray or grayish halite is the other main lithology in these cores. Crystal size is more variable in the

gray halite. Non-halite constituents are visually estimated to locally range from 2-3 % but are more commonly 1% or less. Sulfate and gray clay are both present, and I estimate sulfate is the greater part. The non-halite constituents are unevenly distributed and they are generally intercrystalline. [Clay or fine clastic sediment is normally only found within halite crystals in zones of displacive growth in unlithified sediment. The cores examined did not form this way.] Fluid inclusion pores on the core surface can be ~6 mm (0.25 inch) in one dimension.

Core from 105 (SNLCH105-3&4) displays weak stratification of orange and gray halite (Figure 4). Gray halite is estimated to have more clay and sulfate. The orange halite is interpreted as the initial halite deposit and the gray halite is likely local synsedimentary solution and re-precipitated halite with additional sulfate.

The core segment SNLCH106-8 (Figure 5) encountered a zone of very coarse (to 10 cm; 4 inches) clear halite within the orange halite. The clear halite has larger crystals than the orange halite, and there is no discernible sulfate or clay within the clear halite. Here the clear halite is interpreted as cement filling a vertical synsedimentary dissolution pipe (Figure 8).

"Argillaceous" Halite Cores

The argillaceous halite core segments examined are SNLCH201-4, SNLCH210-7, -8, and -9. These segments display two main halite lithologies and several distinctive features.

The main halite lithologies are coarse, gray halite and fine, light brown halite (Figure 6).

Gray halite includes both anhydrite and clay; these are unevenly distributed. They are found as blebs at the intersection of halite crystals or as irregular stringers that are subhorizontal and planar to curved (Figures 7A and 7B). The halite tends to be translucent, with some large fluid inclusions (3-4 mm; 0.12-0.16 inch).

Fine halite manifests in the core (Figure 6) as irregular masses with indistinct boundaries and low (<0.5%) non-halite components. Distinctive borders with increased insolubles were noted in many of the analogous podular zones in MU-0 and similar intervals in the Salado.

Comparison With Depositional Cycles

As noted in the introductory comments, basic lithologies of the halite beds have been noted for the Salado through earliest WIPP work and by investigators not associated with WIPP. A variety of features and their relationships to the desiccating-upward cycle are related in Holt and Powers (1990, 2011) as well as in Lowenstein (1988). Lowenstein (1988) is particularly notable for discussion of microscopic and other small features.

Soon after mapping of WIPP mined areas began (e.g., TSC-D'Appolonia, 1983), local disruptions were noted in the generally continuous bedded halite of the Salado. Powers and Hassinger (1985) published a brief account of these features, noting that they were truncated by overlying beds and were therefore synsedimentary. Holt and Powers (1990, 2011) had described these features through most of the depositional cycles of the Salado and interpreted them as syndepositional dissolution pipes that were created as the brine table dropped, exposing the surface of the halite pan. Subsequent rises in the brine table caused very coarse, clear halite to cement these pipes (Figure 8). These pipes can be several meters deep, crossing more than one depositional cycle, if the brine table dropped sufficiently.

These pipes develop from exposure surfaces, and the most developed exposure surfaces are frequently at or very near the top of a depositional cycle. They can penetrate the lower part of the depositional cycle that forms the "cleaner" halite in deeper brine. The clear halite in orange "clean" halite of Figure 5 is interpreted as an example of a pipe.
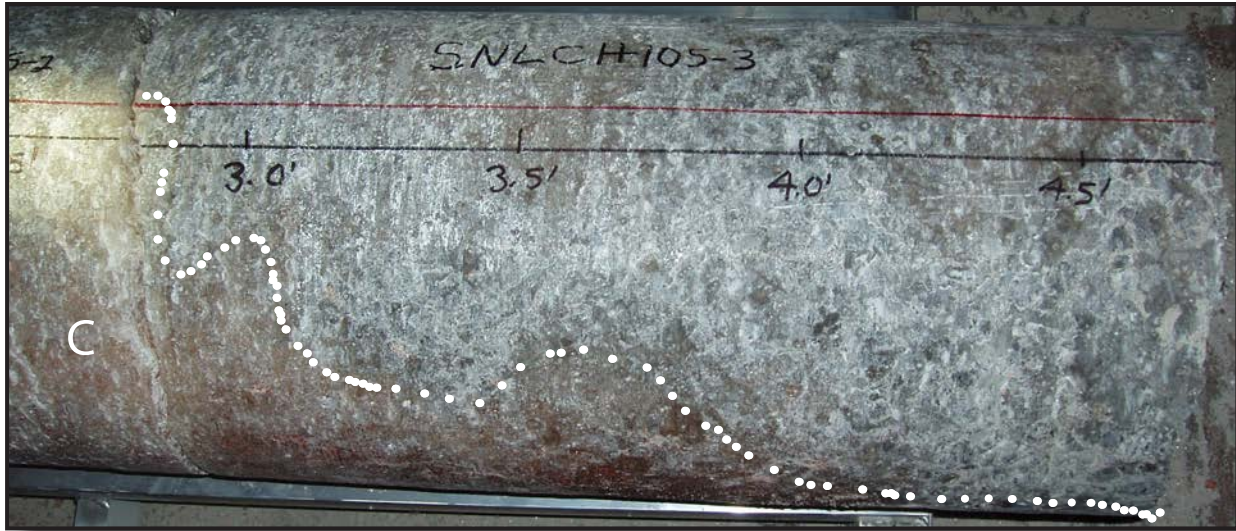
Information Only

Figure 4. Apparent stratification between "clean: halite (C) and gray halite. Red and black lines mark the top of the core. Depth markers are in feet from the rib (wall). Horizontal core. Photo courtesy of SNL.
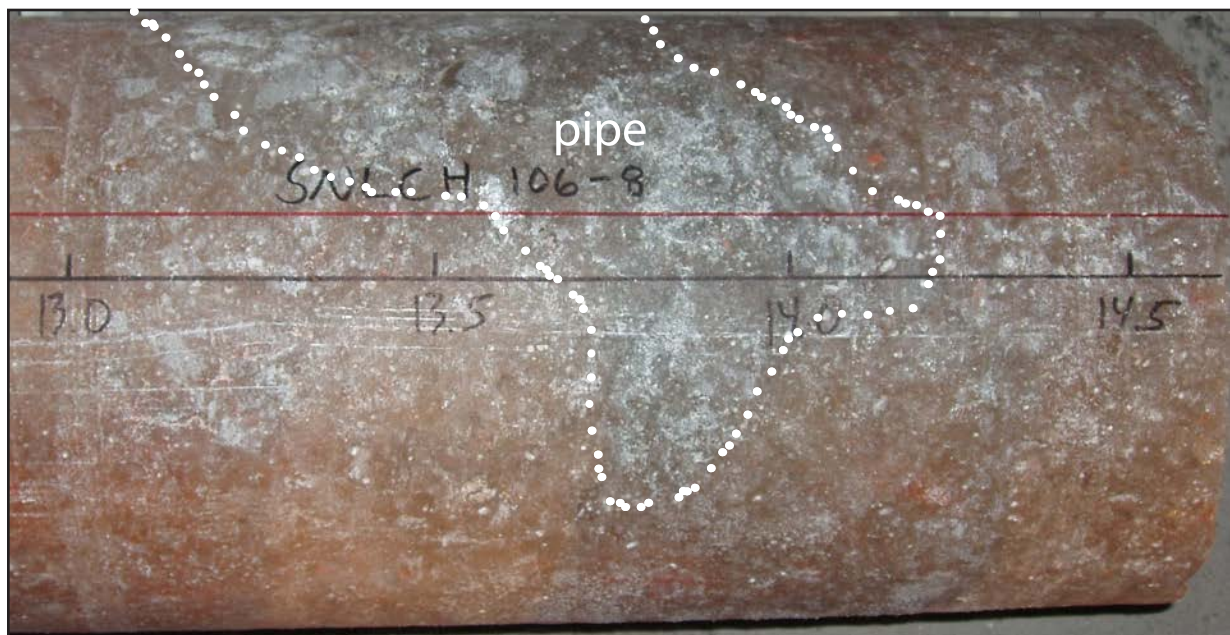

Figure 5. Clear, very coarse halite interpreted as halite cement that filled a synsedimentary dissolution pipe (pipe) vertically into the orange halite of MU-3. Red and black lines are on the top of the horizonatal core. Depth markers are in feet from the rib (wall). Photo courtesy SNL.

Near the end of a desiccating-upward cycle, subaerial exposure dominates the halite pan. Efflorescent salts develop and are finely crystalline and opaque. Such textures have been noted for Death Valley (see references list in Holt and Powers, 2011) in association with dissolution pipes. I associate the fine crystalline, opaque halite from MU-0 (Figure 6) with this process. Holt and Powers (1990) noted larger textures in which masses of this salt resemble pods or nodules (whence "podular") in this upper part of the depositional cycle.

Other features near the top of some desiccating-upward cycles include saucers and desiccation cracks. MU-4 (clay "f"), for example, is notable for these features in some areas (Holt and Powers, 2011), and the discontinuous, subhorizontal clay stringers noted (Figures 7A and 7B) are examples of mini-saucers observable underground where MU-0 is exposed. No desiccation cracks were identified in the examined cores, but they are observable in MU-0 and MU-4 at WIPP.

A copy of Holt and Powers (2011) is attached to this report (Appendix A) for easy reference to features.

SDI Core Examination

Munson et al. (1989) proposed that halite within the reference stratigraphy could generally be assigned as argillaceous halite, with the exception of beds (MU-9, -10, & 12) above and below "anhydrite a." These "clean halite" beds were exposed in the ribs of Room D and other test rooms between N1100 and N1400. At this time, up and down cores through the reference stratigraphy near these test areas are not known to be available for examination, and readily available core descriptions are limited.

Up and down cores, approximately 50 ft in length, were taken from excavations related to SDI from N780, E1310. This location is approximately 500 ft from the south end of Room D, for example (N1100, E1690). Late April 2016, I was able to look at these cores, courtesy of SNL and Los Alamos National

Figure 6. Mixed coarse, gray, translucent halite with fine, light orange to light brown, opaque efflorescent halite (eff) of MU-0. Red and black lines are on the top of the horizontal core. Depth markers are in feet from the rib (wall). Photo courtesy SNL.

Laboratories. Wayne Stensrud (NWP – Geotechnical Engineering) originally described these cores (Appendix B) and was able to be present for part of my examination.

Mr. Stensrud recorded observations clearly with respect to depths, recovery, RQD, and lithology and used standard WIPP forms. These were made available to me ahead of time to review and estimate those intervals of most interest for review. I found the record to be very good; I mainly recorded specific features, verified existing descriptions, and noted the distribution of non-halite components from some units. These notes are included in typed format on the pdf of original field records (Appendix B) and include a red line indicating intervals examined in more detail.

Core recovery was variable but good. The core has been sleeved in plastic that was heat sealed and preserved in standard core boxes. I was able to view textures and basic lithology through the plastic in most cases, and I was able to open, examine, and photograph features for intervals selected to verify common lithologies, features, and transitions.
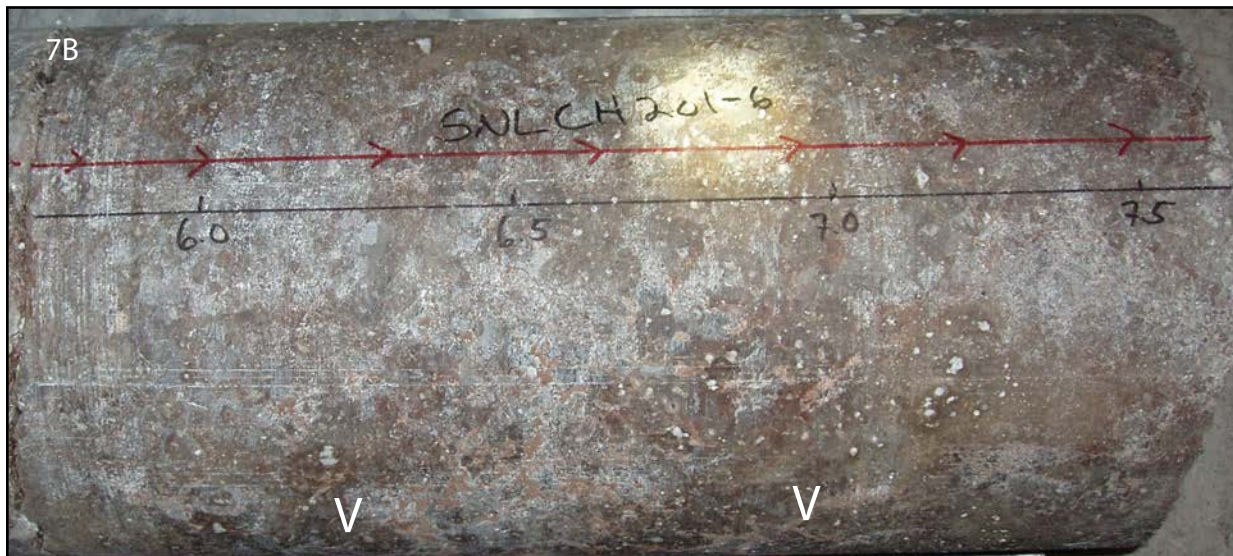
Figure 7. A. End of core from MU-0 showing both disseminated clay blebs and irregular curving thin stringers (V). B. Side view of core with discontinuous subhorizontal clay stringers (V). Red and black lines indicate top of core. Depth from rib is in feet. Photos courtesy of SNL.

Information Only

SDI-BH-00004

The down hole at the SDI location is ~15.5 m (50.6 ft) deep (Figure 9). It begins ~ 1 m (3.5 ft) above Marker Bed (MB) 139. The reported elevation of collar for this hole is ~393 m (1290.52 ft).

The core downward reveals that there is no interval of significance that would visually be designated as "argillaceous halite." The halite beds range from very pure (hardly any visible polyhalite) to those with traces of clay and some small amount of polyhalite.

Clay E was found below MB 139. Clay D was found at a depth of ~4.2 m (13.7 ft), overlying polyhalitic halite with a trace of visible clay. Clay B was recovered from below "anhydrite C" at a depth of ~9.1 m (29.90 ft). A sub-horizontal clay interbed at ~6.7 m (22.05 ft) is ~6 mm (¼ inch) thick, and the core separated along the clay. This is probably clay C.

SDI-BH-00005

The up hole at the SDI location is ~15.5 (50.8 ft) deep. It begins in MU-6, ~2.1 m (7.0 ft) below anhydrite b (Figure 9). The reported elevation for the collar of this hole is ~397.7 m (1304.85 ft).

The up hole encountered reference strata at depths (heights) consistent with other locations underground at WIPP. Anhydrite b is ~2.1 m (7.0 ft) above the collar, underlain by clay G. Anhydrite a is ~3.95 m (12.95 ft) above the collar, and clay H is preserved beneath it. MB 138 is ~10.85 m (35.6 ft) above the collar, and clay K is preserved below it.

Halite beds up to ~6.5 m (21.45 ft) above the collar of the drillhole are variably slightly polyhalitic with traces of clay.

The interval from ~6.5-7 m (21.45-22.9 ft) (MU-14?) is more argillaceous than the underlying beds. A clay-filled desiccation crack was cored at the top of the interval. This is approximately the position of clay I above anhydrite a, but it is thin in other areas.

Argillaceous halites from ~8.4-8.8 m (27.65-28.85 ft) (AH-1) and ~9.3-10.9 m (30.6-35.6 ft) (AH-2) are part of the standard reference stratigraphy. Clay K, at the top of AH-2, underlies MB 138.

Clay content increases in the upper part of H-7, from ~12.5 m (41.0 ft) through AH-3 (~13.6-14.3 m; 44.7-46.85 ft). AH-3 is more argillaceous, easily identified as a unit. The upper part of H-7 appears to be transitional to a more commonly recognizable argillaceous halite bed.

The general comparison to the reference stratigraphy for both cores is very good. The upward core, however, includes two zones (MU-14 and upper H-7) that appear to be
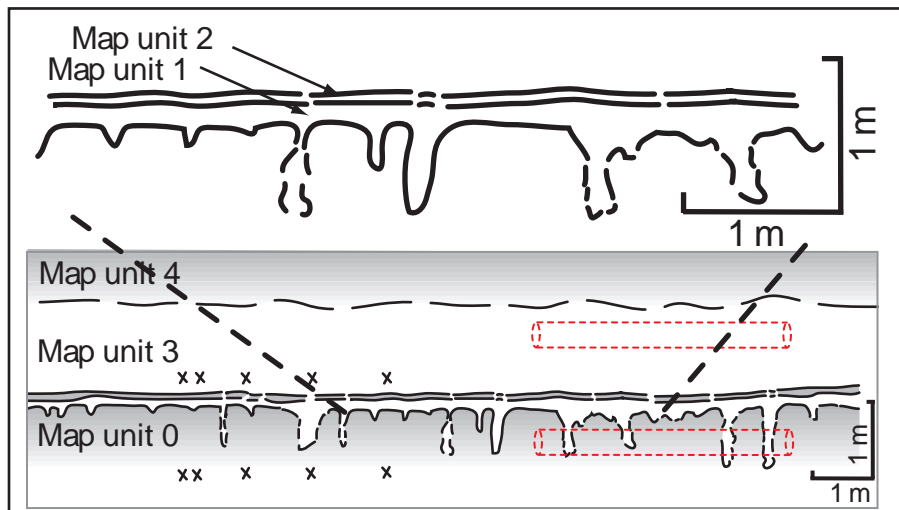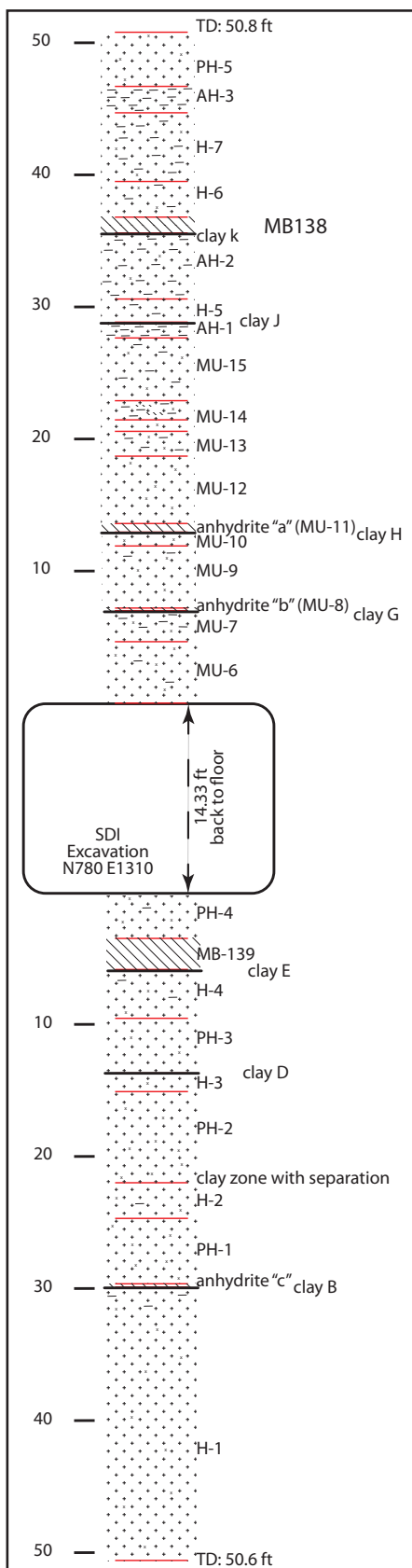

Figure 8. Mapped dissolution pipes in MU-0 S90 drift (Powers, 2000; Holt and Powers, 2011). Large-diameter cores for SNL are roughly located and scaled (red dashed cylinders) for argillaceous (MU-0) and clean (MU-3) halite. Note MU-0 dissolution pipes.

Stratigraphic column (left, depth in ft):

- TD: 50.8 ft
- 50 — PH-5
- AH-3
- H-7
- 40 — H-6
- clay k — MB138
- AH-2
- 30 — H-5
- AH-1 — clay J
- MU-15
- MU-14
- 20 — MU-13
- MU-12
- anhydrite "a" (MU-11) clay H
- MU-10
- 10 — MU-9
- anhydrite "b" (MU-8) clay G
- MU-7
- MU-6
- SDI Excavation N780 E1310 — 14.33 ft back to floor
- PH-4
- MB-139 clay E
- H-4
- 10 — PH-3
- H-3 — clay D
- PH-2
- 20 — clay zone with separation
- H-2
- PH-1
- 30 — anhydrite "c" clay B
- 40 — H-1
- 50 — TD: 50.6 ft

more argillaceous than the standard reference stratigraphy would indicate. The first ~8.5 m (28 ft) of this core (up to AH-1) is mainly halite with low clay content.

Concluding Remarks

The main conclusions here are that the "clean" halite and "argillaceous" halite are visually distinctive at the mine-scale and scale of both large-diameter horizontal cores and the vertical, smaller cores.

Absolute concentrations of water-insoluble (mainly sulfate and silicates) and EDTA-insoluble (mainly silicates) minerals from both lithofacies differ modestly in general, but few quantitative results are available. This is a limitation on assessing the differences. An excellent study of clays within the repository horizon by Krumhansl et al. (1990) unfortunately did not compare the mass of clays from "argillaceous" halite to "clean" halite.

Visual estimates tend to confirm that clay is more abundant in the "argillaceous" halite than in "clean" halite. For the most part, the estimates of clay content that I make visually differ by <~1% up to ~3% or so, although the two lithofacies side-by-side contrast well.

I do not know of any study systematically and quantitatively comparing the distribution of clays and other non-halite components within depositional cycles. Holt and Powers (1990) provide considerable descriptive data of estimated percentage of components and crystal size within depositional cycles. The data on local distribution are not uniform.

What can be readily noticed both through mapping and through examination of these cores is that heterogeneity is related to scale. Small samples (cm-dm) may be fairly

Figure 9 Basic lithology and mapping units of the up and down holes in the SDI. Depth references are in ft. Standard symbols (\\ for anhydrite, + for halite, x for polyhalite, - - for clay).

14

homogeneous within the sample but not very like another sample from < 1 m laterally or vertically. At the mine-scale, mapping units tend to appear more homogeneous. This is not a generalization to all geologic units, but the depositional system that produced the Salado was reasonably massive, leading to considerable lateral continuity and, in this case, repeatable ("cyclic") lithologies and features.

This study does not sustain the assessment of Munson et al. (1989) that all of the halite within the reference stratigraphy, with the exception of halite above and below anhydrite a, could or should be treated as argillaceous halite. The geological distinctions can be made visually with confidence with adequate sampling, based on my experience; whether it matters for mechanical processes is a different concern.

There appears to be sparse data in which the weight percent of clay can be compared to mechanical behavior.

It would seem appropriate to determine if samples from past testing can be recovered for such measures. In addition, I recommend that future samples for mechanical testing be more fully characterized regarding the distribution of non-halite components, as pre-testing fabrics may be important. As demonstrated by descriptions of large-diameter cores taken horizontally through a designated argillaceous halite unit (MU-0), lateral variations can be dramatic because of depositional processes such as dissolution pipes.

The large diameter cores still held by SNL are appropriate for further testing. Either fabrics and distributions should be carefully mapped before sub-sampling, or a geologist should work carefully with rock mechanics investigators to assure such properties are accounted for visually before various stress tests are conducted. Post-test sampling for non-halite constituents can then be conducted for a thorough understanding of the relationships.

Acknowledgements

References Cited

Bodine, M.W., Jr., 1978, Clay-mineral assemblages from drill core of Ochoan evaporites, Eddy County, New Mexico, *in* Austin, G.S., ed., Geology and Mineral Deposits of Ochoan Rocks in Delaware Basin and Adjacent Areas, Carlsbad, NM: Circular 159, New Mexico Bureau of Mines and MIneral Resources, p. 21-30, Socorro, NM.

Bodine, M.W., and Fernalld, T.H., 1973, EDTA dissolution of gypsum, anhydrite, and Ca-Mg carbonates: Journal of Sedimentary Petrology, v. 43, p. 1152-1156.

Hansen, F.D., Senseny, P.E., Pfeifle, T.W., and Vogt, T.J., 1985, Influence of impurities on the creep of salt from the Palo Duro basin: RSI-0259, RE/SPEC Inc., Rapid City, SD; report prepared for Office of Nuclear Waste Isolation, Battelle Memorial Institute, Columbus, OH.

Hansen, F.D., Senseny, P.E., Pfeifle, T.W., and Vogt, T.J., 1987, Influence of impurities on the creep of salt from the Palo Duro basin: RE/SPEC, Rapid City, SD; report prepared for Office of Nuclear Waste Isolation, Battelle Memorial Institute, Columbus, OH. (http://www.osti.gov/scitech/servlets/purl/7166442).

Holt, R.M., and Powers, D.W., 1984, Geotechnical activities in the waste handling shaft, Waste Isolation Pilot Plant (WIPP) project, southeastern New Mexico: WTSD TME-038, Department of Energy, Carlsbad, NM 88221.

Holt, R.M., and Powers, D.W., 1986, Geotechnical activities in the exhaust shaft, Waste Isolation Pilot Plant: DOE WIPP 86-008, Department of Energy, Carlsbad, NM 88221.

Holt, R.M., and Powers, D.W., 1990, Geotechnical activities in the air intake shaft (AIS): DOE/WIPP 90-051, U.S. Department of Energy, Carlsbad, NM. http://www.ntis.gov/search/product.aspx?ABBR=DE91017780

Holt, R.M., and Powers, D.W., 2011, Synsedimentary dissolution pipes and the isolation of ancient bacteria and cellulose: Geological Society of America Bulletin, v. 123, p. 1513-1523, DOI:10.1130/B30197.1.

Jones, C.L., 1978, Test drilling for potash resources: Waste Isolation Pilot Plant site, Eddy County, New Mexico: U.S. Geological Survey Open-file Report 78-592, v. 1 and 2, Denver, CO.

Jones, C.L., 1981, Geologic data for borehole ERDA-9, Eddy County, New Mexico: U.S. Geological Survey Open-file Report 81-469, Denver, CO.

Krieg, R. D., 1984, Reference stratigraphy and rock properties for the Waste Isolation Pilot Plant (WIPP) project: SAND83-1908, Sandia National Laboratories, Albuquerque, NM.

Krumhansl, J.L., Kimball, K.M., and Stein, C.L., 1990, A review of WIPP repository clays and their relationship to clays of adjacent strata: SAND90-0549, Sandia National Laboratories, Albuquerque, NM.

Lowenstein, T.K., 1988, Origin of depositional cycles in a Permian "saline giant": the Salado (McNutt zone) evaporites of New Mexico and Texas: Geological Society of America Bulletin, v. 100, p. 592-608.

Mellegard, K.D., and Pfeifle, T.W., 1993, Creep tests on clean and argillaceous salt from the Waste Isolation Pilot Plant: SAND92-7291, Sandia National Laboratories, Albuquerque, NM.

Munson, D. E., Fossum, A. F., and Senseny, P.E., 1989, Advances in resolution of discrepancies between predicted and measured in situ WIPP room closures: SAND88-2948, Sandia National Laboratories, Albuquerque, NM.

Powers, D.W., 2000, Task 2, Contract 5987 (WIPP underground test site selection and description): memo to Sandia National Laboratories (J.S. Rath), 10 p. + figures + Appendix, March 31, 2000.

Powers, D.W., and Hassinger, B.W., 1985, Synsedimentary dissolution pits in halite of the Permian Salado Formation, southeastern New Mexico: Journal of Sedimentary Petrology, v. 55, p. 769-773.

Powers, D.W., Lambert, S.J., Shaffer, S E., Hill, L.R., and Weart, W.D., eds., 1978, Geological characterization report, Waste Isolation Pilot Plant (WIPP) site, southeastern New Mexico: SAND78 1596, v. I & II, about 1500 p., Sandia National Laboratories, Albuquerque, NM 87185.

Senseny, P.E., 1986, Triaxial compression creep tests on salt from the Waste Isolation Pilot Plant: SAND85-7261, Sandia National Laboratories, Albuquerque, NM.

Stein, C.L., 1983, Results of mineralogical analyses: memorandum to D. E. Munson, dated August 10, 1983, Sandia National Laboratories.

Stein, C.L., 1985, Mineralogy in the Waste Isolation Pilot Plant (WIPP) facility stratigraphic horizon: SAND85-0321, Sandia National Laboratories, Albuquerque, NM.

TSC-D'Appolonia, 1983, Geologic mapping of access drifts "Double Box" area, Geotechnical Field Data Report No. 5: Waste Isolation Pilot Plant, Carlsbad, NM.

US DOE, 1985, Quarterly geotechnical field data report: DOE-WIPP 218, US Department of Energy, Carlsbad, NM.

Information Only

Appendix A

Document Attached for Easy Reference

On-line version of

Geological Society of America Bulletin

Synsedimentary dissolution pipes and the isolation of ancient bacteria and cellulose

Robert M. Holt and Dennis W. Powers

Email alerting services	click www.gsapubs.org/cgi/alerts to receive free e-mail alerts when new articles cite this article
Subscribe	click www.gsapubs.org/subscriptions/ to subscribe to Geological Society of America Bulletin
Permission request	click http://www.geosociety.org/pubs/copyrt.htm#gsa to contact GSA

Notes

THE
GEOLOGICAL
SOCIETY
OF AMERICA

Information Only

Synsedimentary dissolution pipes and the isolation of ancient bacteria and cellulose

Robert M. Holt[†] and Dennis W. Powers
Department of Geology and Geological Engineering, University of Mississippi, Oxford, Mississippi 38677, USA

ABSTRACT

Coarse, clear halite from synsedimentary dissolution pipes in the Permian Salado Formation in southeastern New Mexico (USA) yielded viable halotolerant bacteria and well-preserved cellulose believed to be Permian in age. Here, we show that geologic and hydrologic conditions have isolated these rocks since Permian time. Pipes were dissolved, most likely along cracks (created by thermal contraction or desiccation) and the boundaries of salt polygons (saucers), on exposed Salado Formation salt-pan surfaces down to the level of the water (brine) table. Macropores developed at the brine level in some horizons. As the water level rose, coarse halite cemented the open space. Fluid inclusions (millimeter-scale) trapped bacteria, which were probably in a spore state, as well as cellulose. Inclusion water from pipes in some cycles may have isotopic values reflecting Permian meteoric water, while other cycles may show evaporated Permian seawater.

Exposure surfaces are more prominent in the upper part of Salado Formation depositional cycles due to basin desiccation, as indicated by cracks and dish-shaped laminae. Clays were concentrated on many exposure surfaces by floods, wind, and dissolution. Dissolution pipes formed from these surfaces, and a synsedimentary age is confirmed by undisturbed overlying halite beds. Salado Formation halite has very low permeability ($\sim 10^{-22}$ m²), effectively preventing significant fluid flow and passage of fluids through the formation, either to recrystallize salt or to introduce modern bacteria. Stratigraphic relationships, halite textures, fluid inclusion chemistry, and hydraulic properties are all consistent with a synsedimentary origin of the dissolution pipes, their crystals, and the bacteria and cellulose recovered from the Salado Formation.

[†]E-mail: rmholt@olemiss.edu

INTRODUCTION

Vreeland et al. (2000) claimed to have cultured Permian-age bacteria preserved in fluid inclusions in coarse, clear halite from the late Permian Salado Formation. The site for the samples yielding bacteria was in the air intake shaft at the Waste Isolation Pilot Plant (WIPP) site in southeastern New Mexico (Fig. 1). Although different beds of the Salado Formation, and halite with different textures, were sampled and tested for viable bacteria, these samples were removed from a synsedimentary dissolution pipe. Dissolution pipes are common throughout the upper Salado Formation (Powers and Hassinger, 1985; Holt and Powers, 1990a, 1990b), and they were deliberately targeted because of larger inclusions (millimeter scale). Coarse, clear halite with larger fluid inclusions has commonly been understood as "recrystallized" and therefore not formed at the same time as bedded halite host rock displaying chevron fluid inclusion bands, which are commonly accepted as "primary."

More recently, Griffith et al. (2008) reported that they recovered well-preserved cellulose from similar large fluid inclusions and also from halite crystals without large fluid inclusions, all taken from samples of coarse halite within dissolution pipes of the Salado Formation. The cellulose is the oldest known macromolecule recovered and directly examined (without biochemical amplification or culturing), providing additional impetus for considering the geological and hydrological evidence for isolation of these rocks since the Permian. We contend that the geological and hydrological context of the pipes and their features are clear evidence that these features are synsedimentary and that the halite crystals and included fluid (and bacteria and cellulose) are also Permian in age.

Hazen and Roedder (2001) commented that the age of the bacteria found by Vreeland et al. (2000) must remain in question because the clear halite is recrystallized, possibly by fluids passing at undetermined times through microfractures that have never been observed (Roedder, 1984; O'Neill et al., 1986). Evaporite minerals formed in salt-pan environments are commonly altered by desiccation and flooding before significant burial, as noted also by Roedder (1984), Lowenstein (1988), and many others. Nevertheless, voids or pores are rapidly cemented by halite, and salt attains very low permeabilities soon after burial (Casas and Lowenstein, 1989), thus limiting fluid movement and contamination. Undisturbed overlying beds show that the pipes are synsedimentary dissolution features, and the halite cements that filled them were protected from contamination by the rock's natural hydraulic properties (Powers et al., 2001b).

These synsedimentary dissolution pipes, their stratigraphic context, and their significance as part of Salado Formation depositional cycles remain little known to the geologic community, and, thus, it is difficult for many to assess their significance to any biological sampling program. Here, we focus on the fundamental questions of geological evidence for a syndepositional origin of dissolution pipes and the hydrogeologic and geochemical evidence for isolation of fluid inclusions since deposition.

MOTIVATION

The claim by Vreeland et al. (2000) is one of many that have been made for bacteria allegedly isolated from halite or brine (see review of earlier work by Grant et al., 1998). Factors that put earlier studies (e.g., Dombrowski, 1963) in question range from sampling to laboratory procedures and, more likely, to general disbelief (Vreeland and Rosenzweig, 2002). Cano and Borucki (1995) cultured a bacterium from the gut of a bee trapped in Dominican amber estimated at 25–30 Ma. Stringent laboratory procedures provided convincing evidence that the bacterium was not from laboratory contamination. While there was no discussion of the geological background of these amber samples, there was an implicit assumption that the material (amber) isolated the organism from
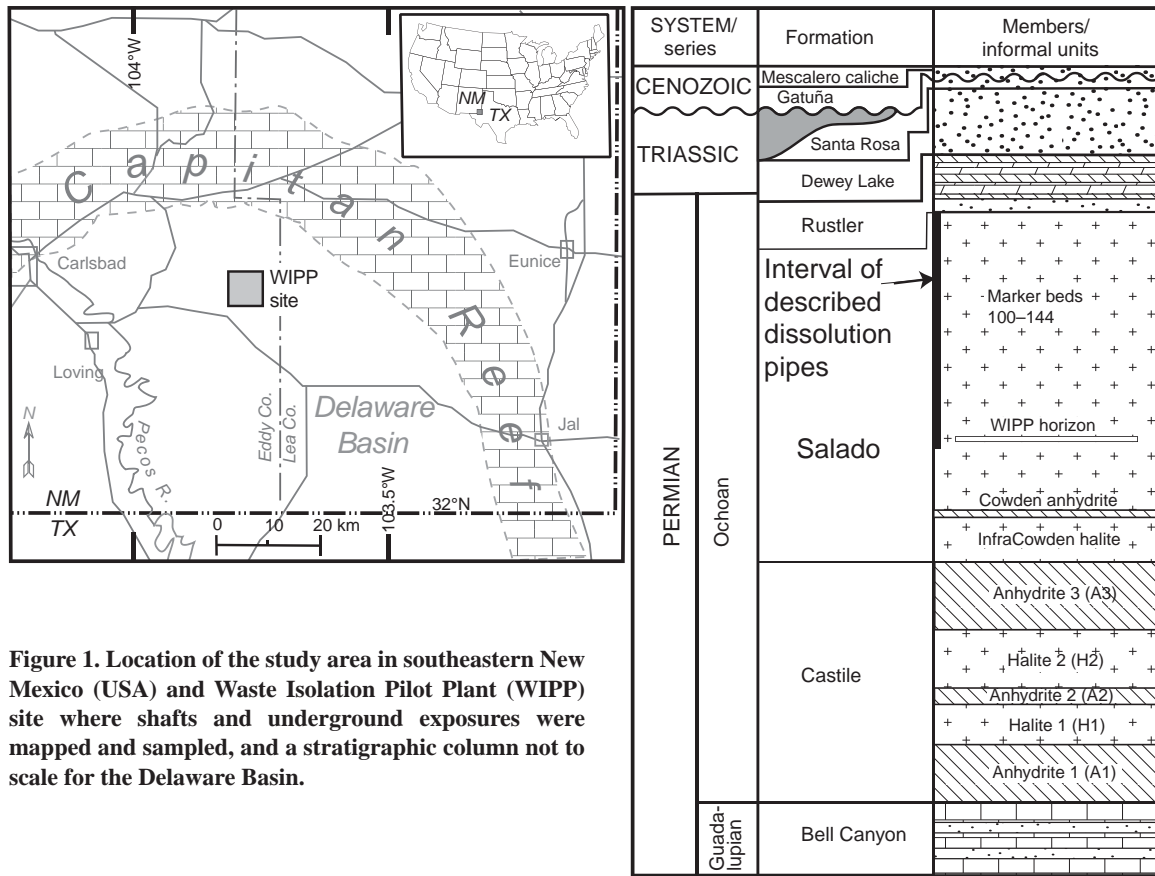
Figure 1. Location of the study area in southeastern New Mexico (USA) and Waste Isolation Pilot Plant (WIPP) site where shafts and underground exposures were mapped and sampled, and a stratigraphic column not to scale for the Delaware Basin.

outside contamination during the time since the amber was deposited. Until the study of Cano and Borucki (1995), evidence of the survival of organisms over geological time was not widely accepted. Recent reports of chloride-bearing surface materials on Mars (Osterloo et al., 2008) raise the prospects of evaporite minerals and rocks hosting life or evidence of life on Mars. Biological studies of Salado Formation halites may guide future efforts to identify life on Mars; geological studies are necessary to establish that the rock remained isolated from contamination prior to sampling.

Grant et al. (1998) listed five requirements to establish an ancient origin for a bacterium in halite: inaccessibility (isolation) of the environment, avoidance of contamination during sampling and culturing, unique characteristics of the organism, repeated culture from related samples, and phylogenetic distinctness. Vreeland and Powers (1998, p. 63) posed three questions to be considered in making a claim that a bacterium has been recovered from a geologically old sample.

1. Did the rock remain isolated from the biosphere during a relevant (geological) period of time?

2. Was the rock contaminated during sampling?

3. Did laboratory techniques maintain sterile conditions during analysis?

Although unique characteristics or phylogenetic distinctness might add excitement to a discovery, it is not safe to assume that all organisms in the modern environment have been discovered and characterized. Vreeland and Rosenzweig (2002) pointed out the inconsistency of using this criterion—a novel bacterium found apparently isolated in an ancient geologic medium might later be discovered in the modern environment.

From a different perspective, Powers et al. (2001a) have hypothesized, for example, that bacteria such as those reported by Vreeland et al. (2000) may be re-introduced into the surface biosphere. Near-surface Salado Formation halite is being dissolved and the brine released continuously into the nearby Pecos River (southeastern New Mexico). The late Cenozoic geological history of this area indicates that this has been occurring for several million years without doubt (Powers and Holt, 1993), and the longer history of southeastern New Mexico geology suggests there may have been other episodes where Salado Formation halite has been dissolved (e.g., Bachman, 1980). Genetic evolutionary rate tests used by Willerslev and Hebsgaard (2005) as an

indicator of age have no established metric for mutation rates over such times (Lowenstein et al., 2005) and may be confounded further by periodic or continuing reintroduction of a "parent" organism into the accessible biosphere. Graur and Pupko (2001, p. 1143 and p. 1145) also applied evolutionary rate tests as "the-proof-of-the-pudding-is-in-the-eating principle," concluding that "the pudding just tastes too fresh to be Permian…." Nickle et al. (2002) also applied such tests, coming to generally similar conclusions as Graur and Pupko (2001). Nickle et al. (2002) more clearly stated some of the assumptions in such tests. They also suggested other lines of examination, reiterating some of the points made by Hazen and Roedder (2001) regarding geological isolation.

A major concern for recovery and analysis of ancient biomaterials is to avoid contaminating the sample during retrieval and analysis. Vreeland et al. (2000) and Rosenzweig et al. (2001) provided details of stringent laboratory protocols and sample handling procedures for Permian bacteria. The cellulose recovered from Salado Formation halite by Griffith et al. (2008) was directly imaged using transmission electron microscopy. While there were processing steps to concentrate the material, there were no

replication steps such as by polymerase chain reaction (PCR) or growth by culturing. This is not a criticism of other studies; it differentiates the process and indicates that original material is available for further analysis. Schubert et al. (2009) used microscopy to observe directly prokaryotes in 30-ka halite from cores from Death Valley and were also able to culture these organisms. Other recent studies (Schweitzer et al., 2007; Asara et al., 2007) reported proteins isolated from Late Cretaceous dinosaur bones, showing again the potential for other environments to preserve such materials intact for geological periods of time.

Whether directly analyzed (e.g., cellulose) or amplified (e.g., deoxyribonucleic acid [DNA]) or grown (e.g., microorganisms), the recovered organisms and organic materials from geologic materials need to be understood in the context of the geology and hydrology of the setting to support claims of isolation from contamination before recovery. That is our objective for this study of the Salado Formation.

STRATIGRAPHIC SETTING FOR THE SALADO FORMATION

In the northern Delaware Basin, the Castile, Salado, Rustler, and Dewey Lake Formations comprise the Ochoan Series (Fig. 1), designated by Adams et al. (1939) and commonly considered late Permian in age (e.g., Hills and Kottlowski, 1983). Fossils are limited in this sequence, although a fauna from the lower Rustler Formation is considered to be Permian in age (Donegan and DeFord, 1950). Schiel (1988, 1994) inferred that the Dewey Lake Formation is likely Triassic, except for the lowermost part, while Lucas and Anderson (1993) asserted that the Dewey Lake Formation is entirely Permian. More recently, Renne et al. (1996) obtained radiometric ages (Ar-Ar) of 249–250 Ma from ash beds in the lower Quartermaster Formation in the Texas Panhandle; the Quartermaster Formation is lithologically similar to the Dewey Lake Formation and is in a similar stratigraphic context. Lithologic contacts are not inherently isochronous, but the particular relationships of the evaporites and red beds across this area suggest relatively close depositional ages. Radiometric ages (^{40}Ar/^{39}Ar) from langbeinite within the Salado Formation of 251 ± 0.2 Ma (Renne et al., 2001) are consistent with an end-Permian deposit.

Although there is uncertainty about the precise age of the Salado Formation and the Ochoan, the Permian–Triassic boundary is very likely to fall within the sequence, probably above the evaporites. Because of this, more detailed studies of the age and depositional environments of these rocks, and the included

biological materials, may provide further information about end-Permian events of worldwide significance.

BASIC SALADO FORMATION GEOLOGY

Most of the Salado Formation consists of repetitive evaporite sequences with characteristics commonly indicating "desiccating upward cycles" (e.g., Holt and Powers, 1990a, 1990b) after initial flooding. Schaller and Henderson (1932) noted that the Salado Formation revealed evidence of increasing evaporation in cycles, resulting in a basic depositional sequence of sulfates to chlorides to bittern salts repeated through the formation. Gard (1968) recorded excellent examples of cracks and polygonal ground in the Salado Formation, noting (p. 10) that, "Desiccation cracks observed at several places … indicate recurrent complete evaporation during deposition of the Salado Formation." Lowenstein (1988) distinguished two types of evaporite depositional cycles based on whether basal carbonate and sulfate beds were present (type I) or not (type II), and he inferred marine or continental water sources, respectively. Holt and Powers (1990a, 1990b) summarized the halite portions of depositional cycles as commonly revealing increasing evidence upward of subaerial exposure (Fig. 2), similar to the saline pan cycle of Lowenstein and Hardie (1985). Diagnostic features for the halitic part of these cycles in the Salado Formation include, from the base up: subaqueous halite that is coarse, mud poor, stratified, and displays some chevron or cornet halite; fine-grained, opaque halite that is variably bedded, and includes some clastic material, particularly outlining blocky to rounded masses ("podular" structures; Holt and Powers, 1990a, 1990b); and fine to coarse, mud-rich halite with saucer- or bowl-shaped bedding (teepees) and thermal contraction or desiccation cracks.

Saucer-shaped bedding or teepees and cracks are unequivocal evidence of desiccation of the saline pan environment. Tucker (1981) analyzed the thermal expansion and contraction of bedded halite and concluded that such cracks and polygons are more likely a consequence of this process than of desiccation. We recognize this as a valid mechanism. The mechanism of crack formation is not important here; the fact that it forms in a desiccating environment (common to both hypothesized origins) is important. Fine-grained, opaque halite that is disrupted into irregular shapes by desiccation and infiltration of clastics is becoming increasingly interpreted as efflorescent halite (e.g., Holt and Powers, 1990a, 1990b; Li et al., 1996; Bobst et al., 2001; Lowenstein et al., 2003), consistent
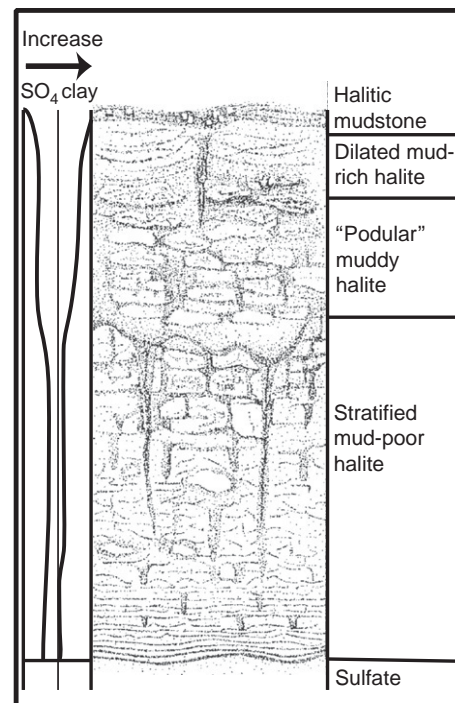
Figure 2. Idealized "desiccating-upward" Salado Formation halite cycle showing increasing pipe size and clay upward, with cracks at some exposure surfaces (modified from Holt and Powers, 1990a, 1990b).

with the interpreted environmental setting for Salado Formation dissolution pipes. Dissolution pipes are also becoming recognized as part of the diagnostic features of the saline pan environment and water-table drops (e.g., Li et al., 1996), although most reports are of the centimeter to decimeter scale observed in cores or thin sections (e.g., Shearman, 1970).

SYNSEDIMENTARY DISSOLUTION PIPES OF THE SALADO FORMATION

Dissolution pipes exposed in the air intake shaft at WIPP illustrate some representative features discussed in this paper (Fig. 3). Dissolution pipes are deeper than they are wide, crosscut depositional features and stratification, and are mainly vertical. Their vertical cross section ranges from vertically elongated to prismatic or channel-like, with the wide end at the top. Boundaries with the host rock range from sharp to diffuse; most of the examples in Figure 3 show relatively sharp boundaries. Dissolution pipes can be related to a common surface in some exposures (e.g., Figs. 3A and 3B). Some areas where pipe development is extensive (Fig. 3C) reveal only residual stacks of the preexisting halite, and these are clues to the existence
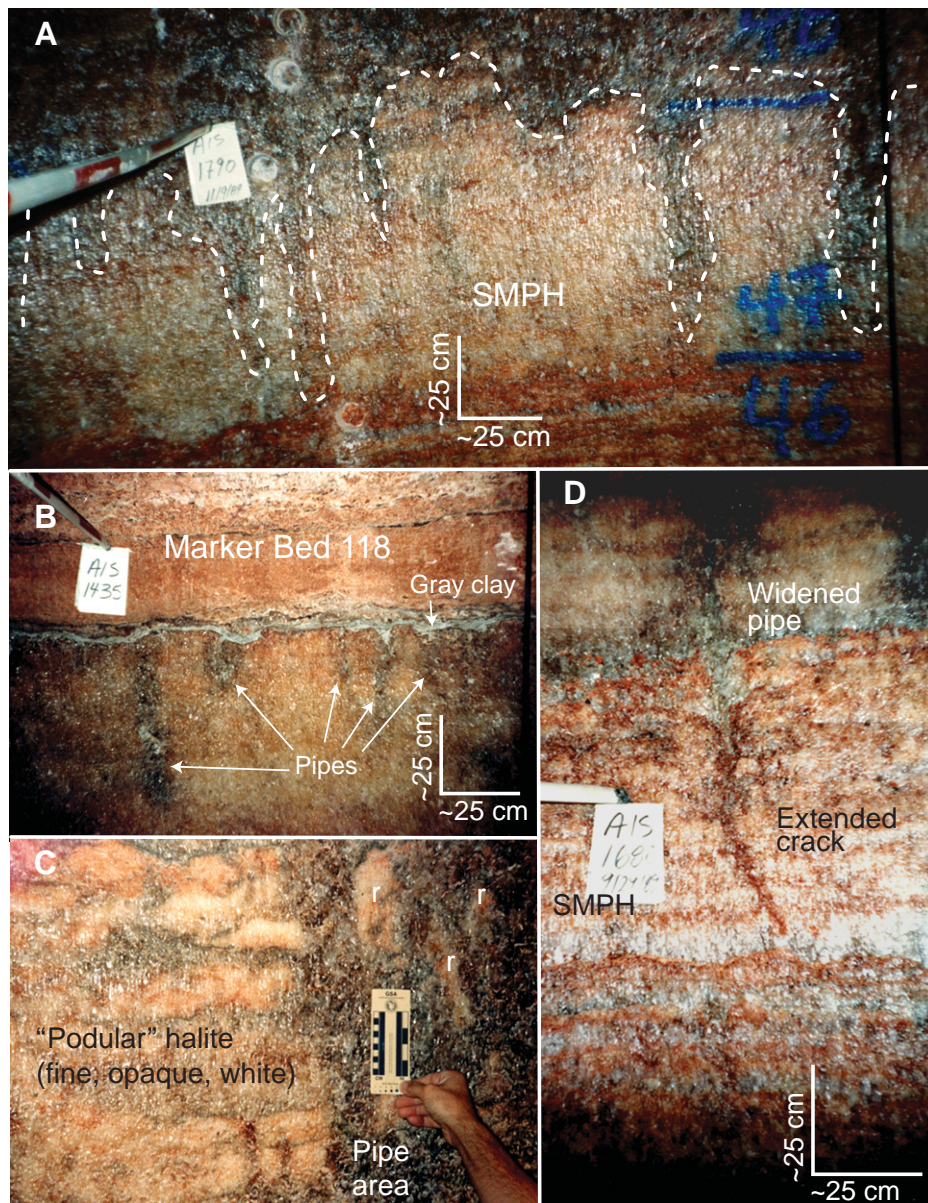
Figure 3. Examples of dissolution pipes from the air intake shaft at Waste Isolation Pilot Plant. (A) Dissolution pipes at 1790 level (546 m) developed from a single exposure surface in stratified mud-poor halite (SMPH). The reddish-brown laminae in the lower part of the photograph are polyhalite, and lighter beds are halite. The halite in pipes is slightly darker because of larger, clear crystals. (B) Dissolution pipes at the 1435 level (437 m) developed from a relatively flat exposure surface before gray clay draped the surface and a thick sulfate bed (Marker Bed 118) was deposited after the salt pan was flooded by fresher water to begin a type 1 cycle. (C) Fine, opaque halite (generally light colored) in the upper part of some depositional cycles (1945 level; 594 m) originated mainly as efflorescent salt. "Podular" textures developed with repeated short-term exposure, and modest infiltration of insoluble material occurred through accessible porosity. The "podular" zone was later disrupted extensively when the water table dropped; coarser, clear (darker) halite filled the pipe area when the water (brine) table rose. Residual podular halite (r) in the pipe area survived local extensive dissolution. The scale (left side) is 10 cm. (D) A crack at the 1680 level (512 m) developed in stratified mud-poor halite (SMPH). The upper part, possibly developed later from another exposure surface, has widened the crack. Other examples also indicate that successive generations of pipes may follow earlier patterns.

of pipes. Our hypothesis that contraction or desiccation cracks may commonly precede development of dissolution pipes is supported by examples in the air intake shaft (e.g., Fig. 3D), but the direct evidence for this proposition was destroyed in most exposures as dissolution proceeded.

Most of the smaller (centimeter to decimeter) pipes are recorded in the midcycle transition from mainly subaqueous to mainly subaerial environments (Fig. 2). Thin (10–20 cm) subaqueous halite beds commonly show fine efflorescent halite (formed during subaerial exposure) at the top, corroded upper contacts, and small pipes. Sulfate laminae or traces of clay commonly mark the start of the next thin halite bed. Some of these smaller pipes are similar to small features described by Shearman (1970) and, more recently, by Li et al. (1996), Schubel and Lowenstein (1997), Bobst et al. (2001), and Lowenstein et al. (2003). The small size of these pipes through the lower to middle parts of the depositional cycle is consistent with general indications of repeated smaller flooding events and shorter periods of desiccation.

Larger pipes in this study are commonly 1–2 m deep (vertical dimension), but they reach ~3 m deep in some units. Most meter-scale pipes developed from the argillaceous halite in the upper part of the depositional cycle (Fig. 2). Mine exposures ~400 m below the top of the Salado Formation illustrate that dissolution pipes are widespread and stratigraphically bounded (Fig. 4). Deeper pipes in map unit (MU) 0 are spaced 1–5 m apart here, with shallow pipes in between; in other areas, the horizontal spacing may reach tens of meters. A rather uniform maximum depth of ~1 m for pipes in MU 0 suggests water-table control. Some beds display macropores at the base level of coexisting pipes, and they also are filled with coarse clear halite (Fig. 5A). Macropores show that porosity was once interconnected, allowing infiltrated freshwater to dissolve salt at the level of the brine table. These features are common in modern salt-pan environments (Fig. 5B). Traction deposits in one pipe near the top of the Salado Formation also indicate that some pipes had significant channel flow (Fig. 6).

Superjacent continuous beds of subaqueous halite (e.g., MU 1, Fig. 4), deposited by flooding at the beginning of a new depositional cycle, are clear evidence of the syndepositional formation of the pipes. MU 2 is brown, slightly argillaceous halite paralleling MU 1. MU 2 shows narrow breaks at a spacing and frequency different from the pipes in MU 0. Some breaks overlie deeper pipes in MU 0. This illustrates a point observed through the Salado Formation—later pipes may follow the same trend and overprint

Figure 4. Map of dissolution pipes in beds ~400 m below the top of the Salado Formation showing areal distribution and consistency of depth. Undisturbed overlying beds are clear evidence of syndepositional age. Some breaks in map unit (MU) 2 coincide with some earlier pipes in MU 0. Argillaceous halite (MU 0, 2, 4) is shaded; coarse halite (MU 1, 3) has no pattern; and the symbol "x" indicates polyhalite.
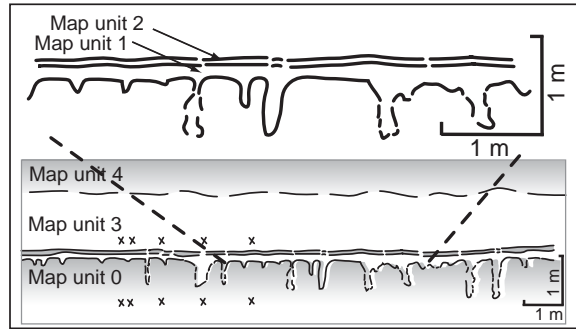
earlier, lower pipes (Fig. 7). If later pipes become large, evidence of earlier pipes will be destroyed. Several generations of pipes can be distinguished within some of the zones, indicating periods dominated even more strongly by subaerial exposure (Fig. 8).

Hundreds of exposure surfaces and associated dissolution pipes are preserved in the upper part of the Salado Formation in the study area. A large-diameter (~6 m) shaft at WIPP displays the features well, and a segment of the shaft map (Fig. 8) illustrates vertical relationships. Lowenstein (1988) suggested meter-scale depositional cycles for the Salado Formation, and the exposure surfaces are consistent with this scale. Mapped relationships demonstrate that larger pipes develop from, or are closely associated with, major exposure surfaces marked by sharp contacts and features described in the next two sections. Upper Salado Formation beds are dominated by two environments: the subaqueous (or phreatic), indicated by stratified, mud-poor halite, and the vadose zone, indicated by efflorescent salt and a variety of exposure features, including dissolution pipes.

Subaerial exposure is indicated in argillaceous halite beds by cracks, dish-shaped cross sections, and concentrated clay on subhorizontal bedding surfaces (Fig. 9). MU 3 and MU 4 illustrate a desiccating-upward cycle, but MU 4 did not develop significant piping. The water table apparently did not drop as far or as long as in some other cycles. Deeper pipes tend to be associated with surfaces with thicker clay, but pipes also developed on subhorizontal surfaces with little or no accumulated clay.

Most depositional cycles in the upper 425 m of the Salado Formation reveal pipes. Pipe frequency and size vary from cycle to cycle, but there is no obvious upward trend in frequency or size.

Figure 5. Types of macropores, from the Salado (A) and a recent analog (B). (A) Macropores, filled with coarse clear halite, are outlined in the vicinity of dissolution pipes associated with thin (10–20 cm) halite beds and laminar sulfate (polyhalite). Macropores are believed to develop at the brine table below the surface when fresher water infiltrates and dissolves halite at the top of the brine table until the fresher water becomes saturated with respect to halite. When the brine table rises, macropores are filled by coarse, slowly grown, halite cements. (B) A large (9 cm diameter), open macropore in halite just above the brine table in the Devil's Golf Course in Death Valley, California. The large, coarse halite crystals at the base of the macropore are incipient macropore cements.

SYNSEDIMENTARY HALITE CEMENTS

Halite cements are ubiquitous in the Salado Formation at a variety of scales and with a variety of morphologies. At the stratum scale, coarse, clear halite cements occupy voids that were created by dissolving halite along the contacts between bottom-growth (chevron) halite or around cumulate halite. Similar features have been well documented in many other thin-section–based studies of halite (e.g., Lowenstein and Hardie, 1985). Other less-well-documented features are readily observed in outcrop-scale exposures of the Salado Formation in WIPP shafts and are discussed herein. Solution lags of clay and sulfate minerals that cap exposure surfaces (e.g., Holt and Powers, 1990a, 1990b) commonly appear dilated or exploded by coarse,

Figure 6. Sketch of a large, dissolution pipe located at a depth of 328 m in the air intake shaft at the Waste Isolation Pilot Plant. The dissolution pipe contains laminated and cross-laminated claystone and small ripples as well as large centimeter-scale displacive halite crystals. Cross-stratification within the pipe indicates relatively high fluid flows within a laterally connected paleokarst network. When the brine table rose, displacive halite crystals grew in the soft sediments.
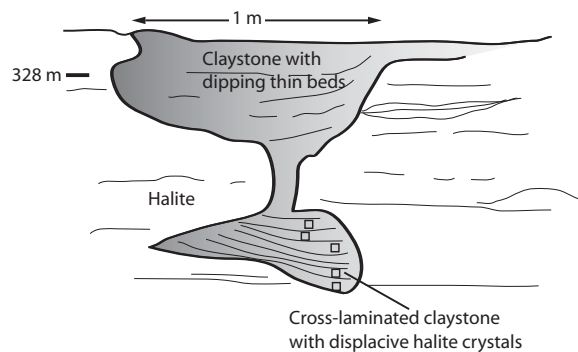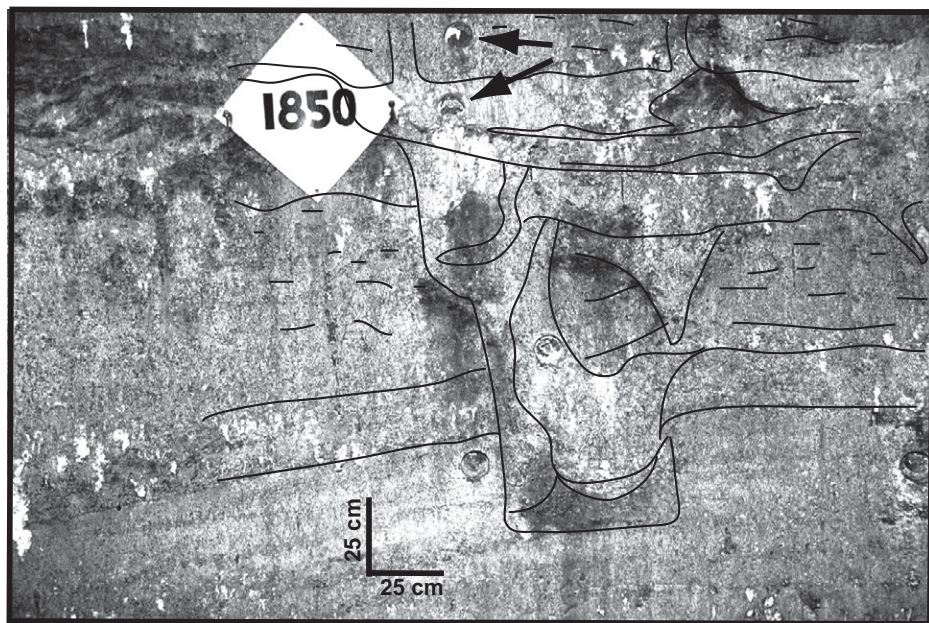
Figure 7. Compound dissolution pipe at 1850 level (564 m) of the air intake shaft shows connections upward to later pipes. Arrows show bacteria sample sites (Vreeland et al., 2000; Satterfield et al., 2002, 2005). Lines accentuate units and features mapped by Holt and Powers (1990a).

clear displacive halite cements (Figs. 10A and 10B). Large (several centimeters across) clear halite crystals fill macropores that are bounded by stratified halite showing chevron fluid inclusion zoning (Fig. 5A). Void space within dissolution pipes is filled with large, clear halite crystals (some exceeding 10 cm across). These crystals commonly show displacive margins with clay and sulfate minerals that accumulated in dissolution pipes (Fig. 10C).

The sedimentological relationships presented here and in Holt and Powers (1990a, 1990b) support a synsedimentary origin for Salado Formation halite cements. Salado Formation halite cements developed within the phreatic zone of the Salado Formation depositional environment, while dissolution pipes and other dissolution features formed in the vadose zone. Clear halite cements overgrew existing halite crystals and passively filled pore spaces in mechanically competent halite, while clear displacive halite crystals grew in more porous sediments, including clay, sulfate minerals, and halite. In some instances, displacive phreatic cements radically overprinted depositional and syndepositional dissolution textures, leading to a dilated appearance. Fluctuating water-table positions relative to the sediment surface led to repeated episodes of vadose zone dissolution and phreatic zone cementation. These processes are particularly effective in modern salt pans, where all visible porosity is occluded at relatively shallow depths (e.g., Casas and Lowenstein, 1989).

RELATED SYNSEDIMENTARY FEATURES

We have found no complete modern analogues to the Salado Formation dissolution pipes, and few ancient features comparable in size are reported. Many pipes are larger than core samples, and "recrystallized" halite is frequently reported without sedimentological context.

Shearman (1970) elegantly described centimeter-scale dissolution pipes formed along boundaries between recent chevron halite crystals and filled with clear halite. Although Shearman calls this clear halite "diagenetic," he relates it to the salt-pan cycle when shallow subsurface brines are concentrated by capillary action and evaporation. A number of ancient examples have now been reported (e.g., Wardlaw and Schwerdtner, 1966; Benison and Goldstein, 2001; Hovorka, 1987; Bein et al., 1991). Hovorka (1987, p. 1035–1036) summarized common features diagnostic of a synsedimentary origin: vertical orientation, relationship to a paleosurface, undisturbed overlying beds, and halite cement fill. Hovorka (1987) noted some geopetal fillings of insoluble minerals.

Salt saucers or polygons with drain holes in Death Valley (USA; Hunt, 1966) and Chilean salars (Stoertz and Ericksen, 1974) may be partial analogues. When the water table is shallow, capillary action forms evaporite minerals (Goodall et al., 2000), and salt pools and

meter-scale surface collapse follow dissolution (Hunt, 1966). Deeper water tables produce solution tubes "presumed to drain downwards to interconnecting fissures that extend to great depths and serve as channelways for subsurface drainage of the basin" (Stoertz and Ericksen, 1974, p. 47).

Similar dissolution pipes, with clear halite cement, are associated with large polygons and contraction cracks in Messinian salt deposits on Sicily (Lugli et al., 1999). A truncating mud layer shows that the features are syndepositional; they formed in a desiccating basin where the water table dropped below the exposed surface (Lugli et al., 1999). Some pipes reached a depth of 6 m below the originating surface. Schreiber and El Tabakh (2000, p. 227) reviewed some studies in which "vertical bedding" features, including cracks and pipes, have been reported and noted that "clear halite from succeeding halite cycles is a common filling."

Watney et al. (2003, p. 129) reported that halite-dominated cycles in the lower Permian Hutchinson Salt Member of the Wellington Formation in Kansas "are capped by erosion surfaces exhibiting karstic pipes and local scallop-shaped dissolution surfaces." The Salado Formation dissolution pipes and pits could be described in this same way.

Rainfall on a depositional surface of the Devonian Prairie Evaporite Formation (Saskatchewan, Canada) developed large drainage channels, hundreds of meters across. These are filled with salt and insolubles, and they lead to low areas on the paleosurface (Baar, 1977). These features may be large examples of some of the Salado features.

Lowenstein and his colleagues have more recently examined similar features from modern saline pan environments and underlying older sediments at Death Valley (e.g., Li et al., 1996), Qaidam Basin of China (e.g., Schubel and Lowenstein, 1997), and Salar de Atacama, northern Chile (e.g., Bobst et al., 2001; Lowenstein et al., 2003). For the most part, dissolution pipes recognized by them are centimeter to decimeter scale because of size limitations of cores. Bobst et al. (2001) and Lowenstein et al. (2003) noted that larger cavities filled with coarse, clear halite occur in efflorescent salt; these are consistent with the scale of larger Salado Formation dissolution pipes described in this paper.

EVIDENCE OF LONG-TERM ISOLATION OF FLUID INCLUSIONS

In the following subsections, we summarize hydrologic, geochemical, radiometric age, and stable isotope evidence supporting long-term isolation of fluid inclusions and bacteria in halite

Figure 8. Dissolution pipes are common in many of the depositional cycles mapped in the air intake shaft at the Waste Isolation Pilot Plant. A section of ~15 m illustrates at least 13 significant exposure surfaces (heavy subhorizontal lines), and many of these have associated dissolution pipes (Holt and Powers, 1990a). Some of the deepest pipes occur near a surface at ~556.5 m below ground level, and the mapped pipes indicate multiple generations of exposure. The dashed line (left column) indicates estimated nonhalite constituents in these cycles, showing that nonhalite constituents increase upward toward the exposure zone. The dotted line shows the relationship between estimated proportions of clay (to the left) and sulfate (to the right) of the nonhalite constituents. This line illustrates that clay commonly increases upward toward the exposure surface, and the sulfate is more common in the subaqueous halite. The horizontal scale of the mapped area is approximate 3–4 m. The basal rock (cross-hatch symbol) is polyhalite.

since 1984 in the vicinity of the WIPP underground excavation, including gas permeability measurements (Stormont, 1997), pressure-pulse tests (Beauheim et al., 1991), constant pressure flow tests (Roberts et al., 1999), and pressure-buildup tests (Roberts et al., 1999). Analyses of these experiments show that the permeability is greatest in a "disturbed-rock zone" that bounds WIPP underground excavations and diminishes over short distances (tens of meters) from the underground opening.

Beauheim and Roberts (2002) summarized the hydrologic investigations of the Salado Formation. They suggested a far-field (outside of the disturbed-rock zone) permeability of $\sim 10^{-22}$–10^{-21} m^2 (hydraulic conductivity of $\sim 10^{-15}$–10^{-14} m/s) and a porosity of ~0.01 for impure halite containing more than a few percent of clay or sulfate minerals. Using percolation theory arguments, Beauheim and Roberts (2002) also suggested that pores in far-field halite containing less than a few percent impurities (e.g., clay or sulfate minerals) are so poorly interconnected that permeability may not exist. Therefore, coarse, clear halite cements in dissolution pipes act as natural, likely impermeable, heterogeneities that limit lateral flow. To illustrate the effectiveness of such low permeability on hydrologic isolation, brine would take ~3–30 m.y. to flow 1 m in argillaceous halite if we assume an unrealistically high hydraulic gradient of 0.01, and assume that Darcy's law is valid for this situation.

Bacterial cells are generally ~0.50 μm in width (Alberts et al., 2002, p. 548), although filterable bacteria 0.2 μm are also reported (e.g., Haller et al., 2000). A study of *Bacillus* sp. spores (Carrera et al., 2006) indicated that spores of *Bacillus subtilis* have mean diameters of 0.48 ± 0.03 μm, which is the smallest of the group. Intercrystalline apertures calculated for reported Salado Formation permeabilities are at least 2–4 orders of magnitude smaller than these bacterial spores, indicating that advective transport is not a viable mechanism for introducing bacterial spores from externally derived fluids.

Far-field pore pressures in the Salado Formation are likely at or very close to lithostatic pressure (Beauheim and Roberts, 2002; Roberts et al., 1999; Holt and Powers, 2010), and drill-stem tests in the Salado Formation showed pressure buildup values indicative of brine levels above the ground surface (Mercer, 1987). This is not surprising because halite is capable of creep deformation and plastic behavior. If the porosity of the Salado Formation were sufficiently interconnected to allow the widespread flow of fluids, Salado Formation fluid would flow upward into the closest overlying aquifer (the Culebra Dolomite Member of the Rustler

cements developed in dissolution pipes. While these are based primarily on observations from the Salado Formation at WIPP, they are consistent with evidence from other areas as well.

Hydrologic Isolation

The rocks of the Salado Formation are generally recognized to be of extremely low permeability, and hydraulic testing in low-permeability materials, like Salado Formation halite, is difficult. Darcy's law may not be applicable in very low-permeability materials under naturally low hydraulic gradients (e.g., Neuzil, 1986), and some researchers (e.g., Swartzendruber, 1962; Pascal, 1981) suggest that low-permeability media may have threshold gradients, below which no flow can occur. Despite these difficulties, a variety of in situ hydraulic tests have been performed
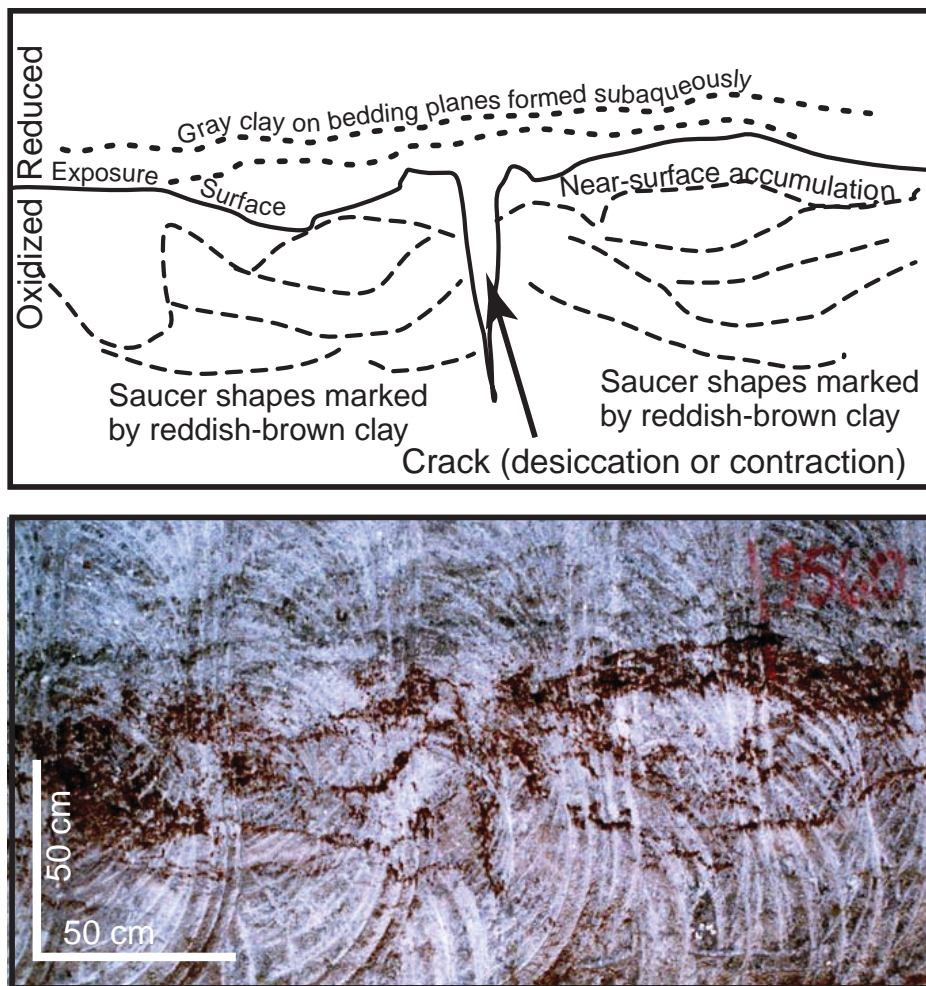
Figure 9. Desiccating-upward cycle is illustrated by a crack at the top of the cycle and clay along saucer shapes. This example is from map unit (MU) 4 (Fig. 4), which is not known to have developed pipes.

Formation halite from several beds showing interbed differences, and they believe the compositions are similar to evaporating modern seawater. Horita et al. (1991, p. 421) also concluded that "inclusion brines in clear parts of the halite samples were derived from the same evaporite brines as those in chevron inclusions." Satterfield et al. (2002, 2005) reported that fluid inclusions from the successful bacterial sampling site in the Salado Formation have ionic concentrations indicating evaporating Permian seawater, and they concluded that the halite cements and their fluid inclusions are synsedimentary. Photomicrographs of fluid inclusions from the bacterial sampling site show no microscopic fractures (Satterfield et al., 2005, archive material) that would indicate injection or passage of externally derived fluids (as postulated by O'Neill et al., 1986).

For a synsedimentary origin of pipes, we expect inclusions from pipe halite to vary chemically from bed to bed, depending on the role of meteoric water in any particular depocycle. Pipe halite inclusions are likely to vary from inclusions in the host bedded halite, as well, although Horita et al. (1991) and Bein et al. (1991) showed some with similar chemistry. Future sampling needs to be carefully directed because inclusion-banded halite may form in pipes during more rapid crystallization. We would expect more homogenization of inclusion chemistry in coarse halite if the halite had been recrystallized by later movement of brines vertically through the formation.

Radiometric Ages

Long-term geochemical isolation is further supported by Salado Formation age dates. The Salado Formation is commonly accepted as Permian in age (e.g., Hills and Kottlowski, 1983). Renne et al. (1998, 2001) obtained $^{40}Ar/^{39}Ar$ plateau ages with an older mode of 251 ± 0.2 Ma from Salado Formation langbeinite at three different stratigraphic levels, and they suggested this is consistent with a depositional age. Lithologic equivalents to the overlying Dewey Lake Formation include tuffs in the lower part of the formation that have dates of 249–250 Ma based on $^{40}Ar/^{39}Ar$ analyses of sanidines (Renne et al., 1996, 2001). Many analyses of Salado Formation mineral and rock samples yield radiometric ages in the range of ca. 200–215 Ma (e.g., Brookins and Lambert, 1987). Renne et al. (2001) also reported plateau ages of ca. 93 Ma from some langbeinite samples. Renne et al. (2001) suggested at least local recrystallization because of the intimate association of langbeinite grains with such widely varying ages. Local recrystallization, however,

Formation) and downward toward the closest underlying aquifer (the Bell Canyon Formation).

In the vicinity of the WIPP, low permeabilities and outward gradients have likely persisted for most of the Salado Formation's postdepositional history. The northern Delaware Basin has been disturbed tectonically very little since the Permian. The main events have been very broad uplifts and exposure since the Triassic, and slight eastward tilting during the mid-Cenozoic (e.g., King, 1948; Bachman, 1980). The Salado Formation in the vicinity of the WIPP shafts shows little structural deformation; well-constrained structure contours of an overlying unit in the Rustler Formation display damped features of deformed Castile Formation in the region (Powers et al., 2003). We analyzed regional depositional patterns and conclude that the Salado Formation was likely buried to its maximum depth by the

close of the Triassic and has been subjected to less than 500 m of unloading due to erosion since that time.

Geochemical Isolation

Chemical analyses from Salado Formation pore fluids and halite fluid inclusions showed substantial variability, consistent with long-term isolation of Salado Formation fluid inclusions from external sources of fluid. Stein and Krumhansl (1988) analyzed 109 large fluid inclusions from one Salado Formation depocycle and found highly variable compositions. They also reported that fluid inclusion compositions differ significantly from Salado Formation pore fluids collected from mine weeps and concluded that fluid movement through the Salado Formation must be extremely limited. Horita et al. (1991) analyzed 49 large inclusions from clear Salado
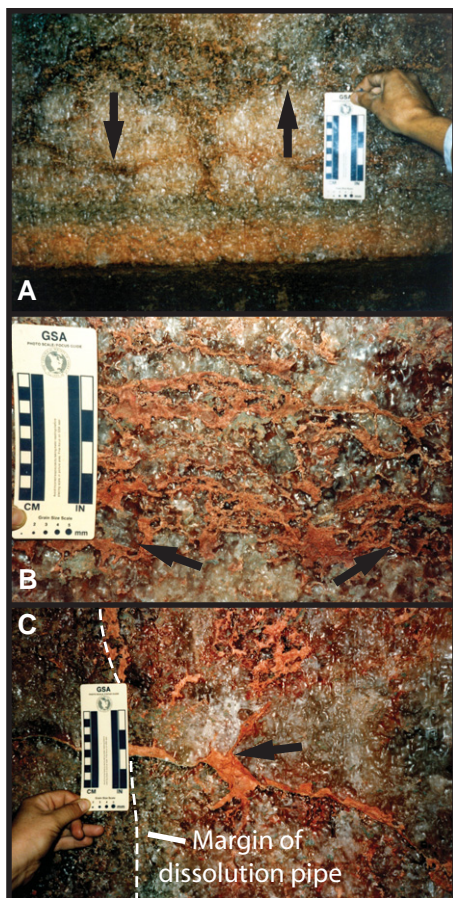
Figure 10. (A) Polyhalite solution lags (orange color) accumulated on exposure surfaces (shown by arrows) are dilated by coarse, clear, displacive halite cements. (B) Dilated solution lags showing displacive halite boundaries; arrows point toward more obvious examples of displacive halite. (C) Large (>10 cm), displacive halite cements within a wide (>0.3 m) dissolution pipe. Note the displacive crystal boundaries with the polyhalite pipe infilling, shown by the arrow.

does not require water, which might contaminate the rocks, from outside the bed or formation. The differences between many radiometric ages of potassium-bearing minerals and the accepted age of the Salado Formation have not been resolved.

Stable Isotopes

Hazen and Roedder (2001) argued that coarse clear halite in the Salado was recrystallized by water moving through the Salado at unknown times, through fractures or microfractures that are not now observed. Stable isotopes from nine large inclusions were interpreted as mixing of modern meteoric water with water derived by dehydrating marine gypsum (Roedder, 1984; O'Neill et al., 1986). O'Neill et al. (1986) also noted, however, that these stable isotope data are consistent with evaporation trends of meteoric water. While these data do not show conclusively that the original water was meteoric, they are very much consistent with the hypothesis that pipes formed on the exposed Salado salt pan. At least in some cases, the influx of unsaturated water was likely to be rainwater and runoff, leading to isotopic values similar to those reported in O'Neill et al. (1986). This contrasts with the actual site of the recovered viable bacterium, where Satterfield et al. (2005) found inclusion chemistry consistent with evaporated Permian seawater. A more systematic approach to the stable isotope analysis of halite filling dissolution pipes in different depocycles is likely to differentiate between flooding by seawater or rainwater and runoff.

SUMMARY COMMENTS

We interpret these halite pipes as synsedimentary and isolated since the Permian based on the stratigraphy, sedimentology, and hydraulic properties of salt. The lithologic sequence and exposure features indicate depocycles were driven by desiccating environments after flooding. Exposed surfaces accumulated clays; and salt saucers, polygons, and cracks developed as the water table dropped below the surface. Rainfall and runoff entered cracks and saucer margins, enlarging them as salt was dissolved. The position of the water (brine) table controlled the depth of pipes and related macropores. When the water table rose, pipes were cemented and sealed by halite crystallizing in a stagnant environment. Renewed flooding deposited regular halite beds above the pipe, indicating the pipes were syndepositional.

The bacterium isolated by Vreeland et al. (2000) is halotolerant rather than halophilic. Bacteria presumably lived in the undersaturated brines that formed the pipes and sporulated as the brine reached halite saturation. The spores were then trapped in fluid inclusions as halite cement filled the pipe.

Inclusion chemistry, radiometric ages, and isotopic analysis show that fluid circulation in Salado Formation halites has been extremely limited since the Permian, consistent with in situ experiments to measure permeability. There is no evidence of postulated microfractures to transmit undersaturated waters through hundreds of meters of evaporites to dissolve and recrystallize the halite after burial. There is also no evidence of larger, through-going fractures that could provide a pathway for contamination.

This mechanism is not practical for hydrological or mechanical reasons, and the chemistry of the brines is not consistent with underlying or overlying formations (Stein and Krumhansl, 1988).

Further studies of rock and inclusion chemistry and isotopic analyses should be useful, however, in unraveling questions about marine versus nonmarine sources of the unsaturated water that dissolves the pipes when sampling is done stratigraphically and in the context of these features within any single depocycle (e.g., Satterfield et al., 2002, 2005). Such sampling may also help to differentiate between depocycles dominated by marine and nonmarine sources of water (as suggested by Lowenstein, 1988).

A further consequence of the work on exposure surfaces and dissolution pipes is that much of the upper Salado Formation formed in, or is overprinted by features of, the vadose zone. The upper parts of these depositional cycles share features that might be expected to develop in some soils, and, like soils, the major part of the geological history is likely contained in the exposure surface and related features rather than in the lower part of the depocycle.

The Salado Formation exposed in the WIPP shafts and underground workings reveals extraordinary preservation of synsedimentary dissolution pipes and the depositional cycles within which they formed. These exposures provide a wonderful opportunity for macroscopic observations regarding cycles, features, and textures associated with very late or possibly end-Permian environments of interest. More precise chemical and isotopic analyses of fluid inclusions and host rocks should yield insights into seawater compositions at this time. The cellulose, if it can be attributed properly to a source, may yield considerable environmental information through stable isotopic analyses. A variety of biologic techniques, ranging from culturing viable organisms to biomarker extraction and analysis, can be applied to single depocycles exposed in mines or through a time series of depocycles in shafts and cores.

Most remarkable of all, the stacked depocycles of the Salado Formation, including the coarse halites of the dissolution pipes, have potential to yield direct data on evolutionary rates, based on bacterial DNA, over geologic stretches of time.

REFERENCES CITED

Adams, J.E., Cheney, M.G., DeFord, R.K., Dickey, R.I., Dunbar, C.O., Hills, J.M., King, R.E., Lloyd, E.R., Miller, A.K., and Needham, C.E., 1939, Standard Permian section of North America: The American Association of Petroleum Geologists Bulletin, v. 23, p. 1673–1681.

Alberts, B., Johnson, A., Lewis, J., Raff, M., Roberts, K., and Walter, P., 2002, Molecular Biology of the Cell (4th ed.): New York, Garland Science, 1548 p.

Asara, J.M., Schweitzer, M.H., Freimark, L.M., Phillips, M., and Cantley, L.C., 2007, Protein sequences from mastodon and *Tyrannosaurus rex* revealed by mass spectrometry: Science, v. 316, p. 280–285, doi: 10.1126/science.1137614.

Baar, C.A., 1977, Applied Salt-Rock Mechanics: Part 1. The In-Situ Behavior of Salt Rocks: Amsterdam, Elsevier, Developments in Geotechnical Engineering 16A, 294 p.

Bachman, G.O., 1980, Regional Geology and Cenozoic History of Pecos Region, Southeastern New Mexico: U.S. Geological Survey Open-File Report 80-1099, 116 p.

Beauheim, R.L., and Roberts, R.M., 2002, Hydrology and hydraulic properties of a bedded evaporite formation: Journal of Hydrology (Amsterdam), v. 259, p. 66–88, doi: 10.1016/S0022-1694(01)00586-8.

Beauheim, R.L., Dale, T.F., and Pickens, J.F., 1991, Interpretations of Single-Well Hydraulic Tests of the Rustler Formation Conducted in the Vicinity of the Waste Isolation Pilot Plant Site, 1988–1989: Albuquerque, New Mexico, Sandia National Laboratories, Report SAND89-0869, 88 p.

Bein, A., Hovorka, S.D., Fisher, R.S., and Roedder, E., 1991, Fluid inclusions in bedded Permian halite, Palo Duro Basin, Texas: Evidence for modification of seawater in evaporite brine-pools and subsequent early diagenesis: Journal of Sedimentary Petrology, v. 61, p. 1–14.

Benison, K.C., and Goldstein, R.H., 2001, Evaporites and siliciclastics of the Permian Nippewalla Group of Kansas, USA: A case for non-marine deposition in saline lakes and saline pans: Sedimentology, v. 48, p. 165–188, doi: 10.1046/j.1365-3091.2001.00362.x.

Bobst, A.L., Lowenstein, T.K., Jordan, T.E., Godfrey, L.V., Ku, T.-L., and Luo, S., 2001, A 106 ka paleoclimate record from drill core of the Salar de Atacama, northern Chile: Palaeogeography, Palaeoclimatology, Palaeoecology, v. 173, p. 21–42, doi: 10.1016/S0031-0182(01)00308-X.

Brookins, D.G., and Lambert, S.J., 1987, Radiometric dating of Ochoan (Permian) evaporites, Waste Isolation Pilot Plant site, Delaware Basin, New Mexico, USA, *in* Bates, J.K., and Seefeldt, W.B., eds., Scientific Basis for Nuclear Waste Management X: Materials Research Society Fall Meeting, Boston, Massachusetts, 1–4 December 1986: Pittsburgh, Pennsylvania, Materials Research Society, v. 84, p. 771–780.

Cano, R.J., and Borucki, M.K., 1995, Revival and identification of bacterial spores in 25- to 40-million-year-old Dominican amber: Science, v. 268, p. 1060–1064, doi: 10.1126/science.7538699.

Carrera, M., Zandomeni, R.O., Fitzgibbon, J., and Sagripanti, J.-L., 2006, Difference between the spore sizes of *Bacillus anthracis* and other *Bacillus* species: Journal of Applied Microbiology, v. 102, p. 303–312.

Casas, E., and Lowenstein, T.K., 1989, Diagenesis of saline pan halite: Comparison of petrographic features of modern, Quaternary and Permian halite: Journal of Sedimentary Petrology, v. 59, p. 724–739.

Dombrowski, H., 1963, Bacteria from Paleozoic salt deposits: Annals of the New York Academy of Sciences, v. 108, p. 453–460, doi: 10.1111/j.1749-6632.1963.tb13400.x.

Donegan, B., and DeFord, R.K., 1950, Ochoa is Permian: The American Association of Petroleum Geologists Bulletin, v. 34, p. 2356–2359.

Gard, L.M., Jr., 1968, Geologic Studies, Project Gnome, Eddy County, New Mexico: U.S. Geological Survey Professional Paper 589, 33 p.

Goodall, T.M., North, C.P., and Glennie, K.W., 2000, Surface and subsurface sedimentary structures produced by salt crusts: Sedimentology, v. 47, p. 99–118, doi: 10.1046/j.1365-3091.2000.00279.x.

Grant, W.D., Gemmell, R.T., and McGenity, T.J., 1998, Halobacteria: The evidence for longevity: Extremophiles, v. 2, p. 279–287, doi: 10.1007/s007920050070.

Graur, D., and Pupko, T., 2001, The Permian bacterium that isn't: Molecular Biology and Evolution, v. 18, p. 1143–1146.

Griffith, J.D., Willcox, S., Powers, D.W., Nelson, R., and Baxter, B.K., 2008, Discovery of abundant cellulose microfibers encased in 250 Ma Permian halite: A macromolecular target in the search for life on other planets: Astrobiology, v. 8, p. 215–228, doi: 10.1089/ast.2007.0196.

Haller, C.M., Rölleke, S., Vybiral, D., Witte, A., and Velimirov, B., 2000, Investigation of 0.2 μm filterable bacteria from the Western Mediterranean Sea using a molecular approach: Dominance of potential starvation forms: FEMS Microbiology Ecology, v. 31, p. 153–161.

Hazen, R.M., and Roedder, E., 2001, How old are bacteria from the Permian age?: Nature, v. 411, p. 155, doi: 10.1038/35075663.

Hills, J.M., and Kottlowski, F.E., coordinators, 1983, Southwest/Southwest Mid-Continent Region: American Association of Petroleum Geologists, Correlation Chart Series, Sheet 18.

Holt, R.M., and Powers, D.W., 1990a, Geologic Mapping of the Air Intake Shaft at the Waste Isolation Pilot Plant: Carlsbad, New Mexico: U.S. Department of Energy Report DOE/WIPP 90–051, 50 p., plus figures and appendices.

Holt, R.M., and Powers, D.W., 1990b, Halite sequences within the Late Permian Salado Formation in the vicinity of the Waste Isolation Pilot Plant, *in* Powers, D.W., Holt, R.M., Beauheim, R.L., and Rempe, N., eds., Geological and Hydrological Studies of Evaporites in the Northern Delaware Basin for the Waste Isolation Pilot Plant (WIPP): Guidebook 14: Boulder, Colorado, Geological Society of America (Dallas Geological Society), p. 45–78.

Holt, R.M., and Powers, D.W., 2010, Evaluation of halite dissolution at a radioactive waste disposal site, Andrews County, Texas: Geological Society of America Bulletin, v. 122, p. 1989–2004, doi: 10.1130/B30052.1.

Horita, J., Friedman, T.J., Lazar, B., and Holland, H.D., 1991, The composition of Permian seawater: Geochimica et Cosmochimica Acta, v. 55, p. 417–432, doi: 10.1016/0016-7037(91)90001-L.

Hovorka, S., 1987, Depositional environments of marine-dominated bedded halite, Permian San Andres Formation, Texas: Sedimentology, v. 34, p. 1029–1054, doi: 10.1111/j.1365-3091.1987.tb00591.x.

Hunt, C.B., 1966, Geochemistry of the saltpan, *in* Hunt, C.B., Robinson, T.W., Bowles, W.A., and Washburn, A.L., eds., Hydrologic Basin Death Valley California: U.S. Geological Survey Professional Paper 494-B, p. B40–B82.

King, P.B., 1948, Geology of the Southern Guadalupe Mountains: U.S. Geological Survey Professional Paper 215, 183 p.

Li, J., Lowenstein, T.K., Brown, C.B., Ku, T.-L., and Luo, S., 1996, The 100 ka record of water tables and paleoclimates from salt cores, Death Valley, California: Palaeogeography, Palaeoclimatology, Palaeoecology, v. 123, p. 179–203, doi: 10.1016/0031-0182(95)00123-9.

Lowenstein, T.K., 1988, Origin of depositional cycles in a Permian "saline giant": The Salado (McNutt zone) evaporites of New Mexico and Texas: Geological Society of America Bulletin, v. 100, p. 592–608, doi: 10.1130/0016-7606(1988)100<0592:OODCIA>2.3.CO;2.

Lowenstein, T.K., and Hardie, L.A., 1985, Criteria for the recognition of salt-pan evaporites: Sedimentology, v. 32, p. 627–644, doi: 10.1111/j.1365-3091.1985.tb00478.x.

Lowenstein, T.K., Hein, M.C., Bobst, A.L., Jordan, T.E., Ku, T.-L., and Luo, S., 2003, An assessment of stratigraphic completeness in climate-sensitive closed-basin lake sediments: Salar de Atacama, Chile: Journal of Sedimentary Research, v. 73, p. 91–104, doi: 10.1306/061002730091.

Lowenstein, T.K., Satterfield, C.L., Vreeland, R.H., Rosenzweig, W.D., and Powers, D.W., 2005, New evidence

for 250 Ma age of halotolerant bacterium from a Permian salt crystal: Reply: Geology, doi: 10.1130/0091-7613(2005)31 (http://www.gsajournals.org/i0091-7613-31-6-e93.pdf).

Lucas, S.G., and Anderson, O.J., 1993, Stratigraphy of the Permian-Triassic boundary in southeastern New Mexico and west Texas, *in* Love, D.W., et al., eds., Carlsbad Region, New Mexico and West Texas: Forty-Fourth Annual Field Conference Guidebook: Socorro, New Mexico, New Mexico Geological Society, p. 219–230.

Lugli, S., Schreiber, B.C., and Triberti, B., 1999, Giant polygons in the Realmonte Mine (Agrigento, Sicily): Evidence for the desiccation of a Messinian halite basin: Journal of Sedimentary Research, v. 69, p. 764–771.

Mercer, J.W., 1987, Compilation of Hydrologic Data from Drilling the Salado and Castile Formations near the Waste Isolation Pilot Plant (WIPP) Site in Southeastern New Mexico: Albuquerque, New Mexico, Sandia National Laboratories, Report SAND86-0954, 39 p.

Neuzil, C.E., 1986, Groundwater flow in low-permeability environments: Water Resources Research, v. 22, p. 1163–1195, doi: 10.1029/WR022i008p01163.

Nickle, D.C., Learn, G.H., Rain, M.W., Mullins, J.I., and Mittler, J.E., 2002, Curiously modern DNA for a "250 million-year-old" bacterium: Journal of Molecular Evolution, v. 54, p. 134–137, doi: 10.1007/s00239-001-0025-x.

O'Neill, J.R., Johnson, C.M., White, L.D., and Roedder, E., 1986, The origin of fluid in the salt beds of the Delaware Basin, New Mexico and Texas: Applied Geochemistry, v. 1, p. 265–271, doi: 10.1016/0883-2927(86)90011-9.

Osterloo, M.M., Hamilton, V.E., Bandfield, J.L., Glotch, T.D., Baldridge, A.M., Christensen, P.R., Tornabene, L.L., and Anderson, F.S., 2008, Chloride-bearing materials in the Southern Highlands of Mars: Science, v. 319, p. 1651–1654, doi: 10.1126/science.1150690.

Pascal, H., 1981, Non-steady flow through porous media in the presence of a threshold gradient: Acta Mechanica, v. 39, p. 207–224, doi: 10.1007/BF01170343.

Powers, D.W., and Hassinger, B.W., 1985, Synsedimentary dissolution pits in halite of the Permian Salado Formation, southeastern New Mexico: Journal of Sedimentary Petrology, v. 55, p. 769–773.

Powers, D.W., and Holt, R.M., 1993, The Upper Cenozoic Gatuña Formation of southeastern New Mexico, *in* Hawley, J.W., et al., eds., Geology of the Carlsbad Region, New Mexico and West Texas: Forty-Fourth New Mexico Geological Society Fall Field Conference Guidebook: Socorro, New Mexico, New Mexico Geological Society, p. 271–282.

Powers, D.W., Holt, R.M., and Powers, E.L., 2001a, Recycling sequestered bacteria through natural hydrogeologic processes [abs.]: Eos (Transactions, American Geophysical Union), v. 82, no. 47, p. F-179.

Powers, D.W., Vreeland, R.H., and Rosenzweig, W.D., 2001b, How old are bacteria from the Permian age?: Nature, v. 411, p. 155–156, doi: 10.1038/35075665.

Powers, D.W., Holt, R.M., Beauheim, R.L., and McKenna, S.A., 2003, Geological factors related to the transmissivity of the Culebra Dolomite Member, Permian Rustler Formation, Delaware Basin, southeastern New Mexico, *in* Johnson, K.S., and Neal, J.T., eds., Evaporite Karst and Engineering/Environmental Problems in the United States: Oklahoma Geological Survey Circular 109, p. 211–218.

Renne, P.R., Steiner, M.B., Sharp, W.D., Ludwig, K.R., and Fanning, C.M., 1996, $^{40}Ar/^{39}Ar$ and U-Pb SHRIMP dating of latest Permian tephras in the Midland Basin, Texas: Eos (Transactions, American Geophysical Union), v. 77, no. 46, p. 794.

Renne, P.R., Sharp, W.D., and Becker, T.A., 1998, $^{40}Ar/^{39}Ar$ dating of langbeinite $[K_2Mg_2(SO_4)_3]$ in Late Permian evaporites of the Salado Formation, southeastern New Mexico, USA: Mineralogical Magazine, v. 62A, p. 1253–1254, doi: 10.1180/minmag.1998.62A.2.320.

Renne, P.R., Sharp, W.D., Montañez, I.P., Becker, T.A., and Zierenberg, R.A., 2001, $^{40}Ar/^{39}Ar$ dating of Late Permian evaporites, southeastern New Mexico, USA: Earth and Planetary Letters, v. 193, p. 539–547, doi: 10.1016/S0012-821X(01)00525-8.

Roberts, R.M., Beauheim, R.L., and Domski, P.S., 1999, Hydraulic Testing of Salado Formation Evaporites at

the Waste Isolation Pilot Plant Site: Final Report: Albuquerque, New Mexico, Sandia National Laboratories, Report SAND98–2537, 276 p.

Roedder, E., 1984, The fluids in salt: The American Mineralogist, v. 69, p. 413–439.

Rosenzweig, W.D., Peterson, J., Woish, J., and Vreeland, R.H., 2000, Development of a protocol to retrieve microorganisms from ancient salt crystals: Geomicrobiology, v. 17, p. 185–192, doi: 10.1080/01490450050121152.

Satterfield, C.L., Lowenstein, T.K., Vreeland, R., and Rosenzweig, W., 2002, The search for microorganisms in brine inclusions in halite: An update: Geological Society of America Annual Meeting Abstracts with Programs, v. 34, no. 6, p. 19.

Satterfield, C.L., Lowenstein, T.K., Vreeland, R.H., Rosenzweig, W.D., and Powers, D.W., 2005, New evidence for 250 million-year age of halotolerant bacterium from a Permian salt crystal: Geology, v. 33, p. 265–268, doi: 10.1130/G21106.1.

Schaller, W.T., and Henderson, E.P., 1932, Mineralogy of Drill Cores from the Potash Field of New Mexico and Texas: U.S. Geological Survey Bulletin 833, 124 p.

Schiel, K.A., 1988, The Dewey Lake Formation—End Stage Deposit of a Peripheral Foreland Basin [M.S. thesis]: El Paso, University of Texas at El Paso, 181 p.

Schiel, K.A., 1994, A new look at the age, depositional environment, and paleogeographic setting of the Dewey Lake Formation (Late Permian?): West Texas Geological Society Bulletin, v. 33, no. 9, p. 5–13.

Schreiber, B.C., and El Tabakh, M., 2000, Deposition and early alteration of evaporites: Sedimentology, v. 47, supplement 1, p. 215–238, doi: 10.1046/j.1365-3091.2000.00002.x.

Schubel, K.A., and Lowenstein, T.K., 1997, Criteria for the recognition of shallow-perennial-saline-lake halites based on recent sediments from the Qaidam Basin, western China: Journal of Sedimentary Research, v. 67, p. 74–87.

Schubert, B.A., Lowenstein, T.K., Timofeeff, M.N., and Parker, M.A., 2009, How do prokaryotes survive in fluid inclusions in halite for 30 k.y.?: Geology, v. 37, p. 1059–1062, doi: 10.1130/G30448A.1.

Schweitzer, M.H., Suo, Z., Avci, R., Asara, J.M., Allen, M.A., Arce, F.T., and Horner, J.R., 2007, Analyses of soft tissue from *Tyrannosaurus rex* suggest the presence of protein: Science, v. 316, p. 277–280, doi: 10.1126/science.1138709.

Shearman, D.J., 1970, Recent halite rock, Baja California, Mexico: Institute of Mining and Metallurgy Transactions, v. 79, p. 155–170.

Stein, C.L., and Krumhansl, J.L., 1988, A model for the evolution of brines in salt from the lower Salado Formation, southeastern New Mexico: Geochimica et Cosmochimica Acta, v. 52, p. 1037–1046, doi: 10.1016/0016-7037(88)90258-X.

Stoertz, G.E., and Ericksen, G.E., 1974, Geology of Salars in Northern Chile: U.S. Geological Survey Professional Paper 811, 65 p.

Stormont, J.C., 1997, Conduct and interpretation of gas permeability measurements in rock salt: International Journal of Rock Mechanics and Mining Science, v. 34, paper 303.

Swartzendruber, D., 1962, Non-Darcy flow behavior in liquid-saturated porous media: Journal of Geophysical Research, v. 67, p. 5205–5213, doi: 10.1029/JZ067i013p05205.

Tucker, R.M., 1981, Giant polygons in the Triassic salt of Cheshire, England: A thermal contraction model for their origin: Journal of Sedimentary Petrology, v. 51, p. 779–786.

Vreeland, R.H., and Powers, D.W., 1998, Considerations for microbiological sampling of crystals from ancient salt formations, *in* Oren, A., ed., Microbiology and Biogeochemistry of Hypersaline Environments: Boca Raton, Florida, CRC Press, p. 53–73.

Vreeland, R.H., and Rosenzweig, W.D., 2002, The question of uniqueness of ancient bacteria: Journal of Industrial Microbiology and Biotechnology, v. 28, p. 32–41.

Vreeland, R.H., Rosenzweig, W.D., and Powers, D.W., 2000, Isolation of a 250-million-year-old halotolerant bacterium from a primary salt crystal: Nature, v. 407, p. 897–900, doi: 10.1038/35038060.

Wardlaw, N.C., and Schwerdtner, W.M., 1966, Halite-anhydrite seasonal layers in the Middle Devonian Prairie Evaporite Formation, Saskatchewan, Canada: Geological Society of America Bulletin, v. 77, p. 331–342, doi: 10.1130/0016-7606(1966)77[331:HSLITM]2.0.CO;2.

Watney, W.L., Nissen, S.E., Bhattacharya, S., and Young, D., 2003, Evaluation of the role of evaporite karst in the Hutchinson, Kansas, gas explosions, January 17 and 18, 2001, *in* Johnson, K.S., and Neal, J.T., eds., Evaporite Karst and Engineering/Environmental Problems in the United States: Oklahoma Geological Survey Circular 109, p. 119–147.

Willerslev, E., and Hebsgaard, M.B., 2005, New evidence for 250 Ma age of halotolerant bacterium from a Permian salt crystal: Comment: Geology, doi: 10.1130/0091-7613(2005)31 (http://www.gsajournals.org/i0091-7613-31-6-e93.pdf).

Appendix B

Scanned Copies of Borehole Logs for

SDI-BH00004
and
SDI-BH0005
Originals Prepared by Wayne Stensrud
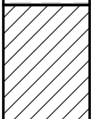
Additional Text and Markings by
Dennis W. Powers
May 2016

Basic Symbols in Core Logs

Symbol   *Description*

Halite; halitic where symbols are scattered

Claystone; argillaceous where symbols are scattered. Clay seam or thin layer indicated by heavy line

Anhydrite; anhydritic if // are scattered

Attachment 1 – Core Log

CORE LOG		Sheet _1_ of _13_

Hole ID: **SDI-BH-00004**   Location: **N780 E1310**

Drill Date: **1/6/14 - 1/8/14**	Drill Method: **Revers Rotary**	Drill Make/Model: **ATLas CopCo Dommec 264**
	Hole Diameter: **4·5/8"**	Barrel Specs: **~4 5/8 x 3 3/4 ID**
Drill Crew: **Blas, Heime Troy**	Hole Depth: **50·6 ft**	Drill Fluid: **Air**
	Hole Orient: **Vertkal Down**	Core Preserv: **Celophane Heat Seal**

Logged by: **Wayne Stensrud**   Date: **1/6/14**   Scale: _____

Survey Coordinates: (Ft)	Northing **10475.38**	Easting **8210.77**	Elevation **1290.52 ft**

Comments: **Core described by Wayne Stensrud, Marked and Preserved by David Gruerin and Brian Dozier With Los Alamos National Laboratories.**

Y6/14 Time	Run Number	Depth (ft)	% Recovered	RQD	Profile (Rock Type)	Description	Remarks
09:12	Run #1	0.0 / 1.0	100%	80%		(0'-3.5') Polyhalitic Halite, Clear to reddish orange, orange-brown to gray Coarse Crystalline, Some medium. Scattered gray Clay, Locally. Contact with lower unit is sharp but irregular and undulating Trace of gray Clay at Contact.	PH-4 clay <<0.01% (only one or two gray blebs) poly is localized as blebs and halite coatings
09:18	Run #2	1.5 / 2.0 / 2.85	100%	10%			no clay; poly blebs larger (up to ~1/2") than higher in cycle, are widely scattered
9:33 / 9:50	Run #3	3.0	100%	59%		(3.5'-5.85') Anhydrite, orange brown to gray. Micro Crystalline Swallow Tail halitic growths Within Anhydrite	MB 139

(Continue data on following page[s], as necessary.)
4.0

Attachment 1 – Core Log

Hole ID: SDI-BH00004	CORE LOG (cont. sheet)	Sheet 2 of 13
Logged by: Wayne Stensrud	Date: 1/6/14	

	Run Number	Depth (ft)	% Recovered	RQD	Profile (Rock Type)	Description	Remarks
1/6/14		4.0					
10:05		4.2				Clay E at base of the Anhydrite. Upper Contact is irregular.	MB 139 (continued)
	Run #4	5.0	100%	27%			
10:20		5.7				— Clay E	
	Run #5	6.0	100%	100%		(5.85'-9.55') Halite. Clear to reddish orange to gray. Coarsely crystalline. Some medium to fine. 1% polyhalite and intercrystalline Clay. Contact with lower unit is gradational based on increased polyhalitic content and grain size.	H-4 trace of clay; gray is mainly anhydrite(?) coarse halite fine halite, tr clay, anhydritic, poly
10:35		6.75					
		7.0					
	Run #6		100%	100%			
		8.0					

Attachment 1 – Core Log

			CORE LOG (cont. sheet)		Sheet 3 of 13

Hole ID: SDI-BH00004

Logged by: Wayne Stensrud   Date: 1/6/14

	Run Number	Depth (ft)	% Recovered	RQD	Profile (Rock Type)	Description	Remarks
1/6/14 Time		8.0					
12:20		8.17			✗	(5.85'-9.55') HaLite (cont)	H-4 (cont)
	Run #7		100%	100%	✗		
		9.0			✗	halite, fine-medium, transparent to opaque; <1% poly in blebs, some tiny films or thin, irregular platelets < 1/2" long; poly broadly distributed, no fabric; no discernible clay	
12:45		9.55			✗		
	Run #8	10.2	100%	78%	✗ ✗ ✗ ✗ ✗	(9.55'- 13.7') Polyhalitic Halite Clear to moderate reddish orange, some gray. Coarsely Crystalline. < 1 to 3% Polyhalite. Contact with Lower Unit is Sharp along clay D, but irregular and undulating.	PH-3 no discernible clay
13:13		10.90 / 1.0			✗		
	Run #9		100%	77%	✗ ✗ ✗ ✗ ✗		
		12.0					

Attachment 1 – Core Log

		CORE LOG (cont. sheet)			
Hole ID: SDI-BH-00004				Sheet 4 of 13	
Logged by: Wayne Stensrud			Date: 1/6/14		

Run Number	Depth (ft)	% Recovered	RQD	Profile (Rock Type)	Description	Remarks
	12.0					
Run #10	12.2 — 13.0		69%	X X X X X X X	(9.55'-13.7') Poly halitic Halite halite, orange, medium-coarse; no clay; ~1% poly as very thin (< 1 mm) subhorizontal stringers and outlines of halite crystals clay D is ~1/32-1/8" thick; truncates halite — Clay D	PH-3 (cont) from 13.57-9.0 ft (upward), orange color (polyhalite?) decreases
12:21						
Run #11	13.57 14.0		73%	X X X X X	(13.7'-15.1') Halite Clear to moderate reddish-orange Medium to Coarsely Crystalline. 1% Polyhalite and gray clay clay. Contact with Lower Unit is gradational based on increased polyhalite Content.	H-3 clay <<1% lower end of H-3; poly mainly in zones as linings around halite
13:40						
1346	14.80					
Run #12	15.0	100%	56%	X X X X X X X	(15.1'-22.0') Polyhalitic Halite Clear to moderate reddis orange 1% to 3% poly halite contact with Lower Unit gradational, based on decreased polyhalitic Content	PH-2 ?
	16.0					

Attachment 1 – Core Log
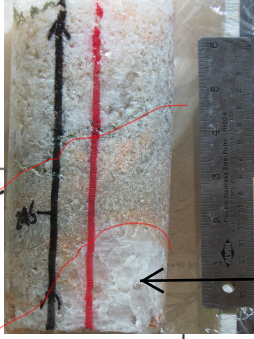
	CORE LOG (cont. sheet)		
Hole ID: SDI-BH-00004			Sheet 5 of 13
Logged by: Wayne Stensrud		Date: 1/6/14	

	Run Number	Depth (ft)	% Recovered	RQD	Profile (Rock Type)	Description	Remarks
1/6/14		16.0					
14:05	Run #13	17.0	100%	58%	x	(15.1'–22.0') Polyhalitic Halite Trace of gray clay Locally	PH-2 (cont)
14:20	Run #14	17.52 / 18.0	100%	29%	x		
14:26 / 1/7/14	Run #15	18.90 / 19.0	100%	0%	x		
		20.0					

clay is nearly non-existent; polyhalite/anhydrite is locally a relatively high % as blebs, also outlines halite crystals; larger fluid inclusions more common in this interval; continues down to 22.0 ft.

Information Only

Attachment 1 – Core Log

		CORE LOG (cont. sheet)					
Hole ID: SDI-BH00004					Sheet 6 of 13		
Logged by: Wayne Stensrud			Date: 1/7/14				

Run Number	Depth (ft)	% Recovered	RQD	Profile (Rock Type)	Description	Remarks
	20.0					
0820 Run #16	20.2	100%	30%	⨯	(15.1'-22.0') Polyhalitic Halite (cont.)	PH-2 (cont.)
	21.0					
0835	21.55					
Run #17	22.0	100%	92%		Low Angled Fracture Clay filled <¼" Thick	
	22.75				(22.05'-24.7') Halite Clear to reddish orange to gray. Medium to Coarsely Crystalline. Some fine Locally Contact with lower unit is gradational. <1% dispersed polyhalite, <1% gray clay and or brown Clay	H-2 zones/beds of fine orange halite with ~2% polyhalite and interbeds of medium-coarse gray halite with little polyhalite or clay; polyhalite is mainly fine crystalline blebs between halite crystals; trace of gray clay or anhydrite at top of polyhalitic zones
Run #18	23.0	100%	100%			
	24.0					

Check

[Typed annotation overlay:] mass of fine polyhalite 21.5 ft below coarse halite and halite with poly stringers; no discernible clay above clay seam. Interpret fracture as secondary.

Attachment 1 – Core Log

		CORE LOG (cont. sheet)			
Hole ID: SDI-BH 00004					Sheet 7 of 13
Logged by: Wayne Stensrud			Date: 1/7/14		

Run Number	Depth (ft)	% Recovered	RQD	Profile (Rock Type)	Description	Remarks

1/7/14

240

24.1'

coarse, gray/orange halite, trace gray clay upward →

24.1

(22.05'– 24.7') Halite

fine-medium gray and → orange halite; no clay

H-2 (cont)

very coarse halite, no clay

24.7'

Run #19 — 100% — 88 — 6%

(24.7'–29.65') Polyhalitic Halite
Clear to Redish orange.
Coarsely Crystalline with
Some medium close to
Lower contact. <1 to 3%
polyhalite, scattered
Anhydrite Stringers.

PH-1
possible displacive(?) halite - thin films of polyhalite around planar halite boundaries

25.0

Run #20 — 100% — 25%

25.35

09:35

26.0

26.75

27.0

thin, irregular polyhalite on halite crystal boundaries; in poorly defined bands

Run #21 — 100% — 66%

polyhalite in more regular, very thin laminae

280

Attachment 1 – Core Log

1/7/14

			CORE LOG (cont. sheet)		
Hole ID: SDI-BH-00004					Sheet 8 of 13
Logged by: Wayne Stensrud			Date: 1/7/14		

Run Number	Depth (ft)	% Recovered	RQD	Profile (Rock Type)	Description	Remarks
	28.0					
Run #22	28.10	100%	50%	x x x x	(24.7'-29.65') Polyhalitic Halite	PH-1 (cont)
	29.0					
	29.31			x x		
Run #23	30.0	100%	78%		(29.65-29.90) Anhydrite. Light to medium gray. Microcrystalline Anhydrite. Scattered Halitic growths. Clay Seam B at Base	Anhydrite "C"
	30.60				(29.90-50.6) Halite. Clear to orange to medium gray and moderate brown. medium to Coarsely Crystalline. Some fine Locally. <1% Polyhalite <1 to 3% brown and gray clay. Argillaceous Halite zones.	H-1 crude 1-3" bands of light brown, fine-medium halite with <1%clay and orange to clear, medium-coarse halite with no clay halite with polyhalite in irregular zones and as outlines of irregular halite crystal surfaces
Run #24	31.0	100%		x x x x x x		
	31.95					
	32.0					

Information Only

Attachment 1 – Core Log

					CORE LOG (cont. sheet)		
Hole ID: SDI-BH-00004						Sheet 9 of 13	
Logged by: Wayne Stensrud					Date: 1/7/14		

Run Number	Depth (ft.)	% Recovered	RQD	Profile (Rock Type)	Description	Remarks
	32.0				(29.90 - 50.6) Halite	H-1 (cont)
Run #25	33.0		100%			
10:56	33.25				clear, coarse halite	
Run #26	34.0		100%		halite, medium-coarse, slightly anhydritic, trace(?) clay	
12:40	34.65				clear, coarse halite	
Run #27	35.0		100%			
12:53	35.90					
	36.0					

Attachment 1 – Core Log

Hole ID: SDT-BH00004		CORE LOG (cont. sheet)			Sheet 10 of 13
Logged by: Wayne Stensrud			Date: 1/7/14		

Run Number	Depth (ft)	% Recovered	RQD	Profile (Rock Type)	Description	Remarks
	36.0					
Run #28	37.0	100%	100%		(29.90'-50.6') Halite	H-1 (cont.)
1310 1317	37.25				very little to no clay above 37.3 ft	
Run #29	38.0	100%	100%			
1322	38.55				halite, fine-coarse; thin beds with 1-3% disseminated clay and poly with some very thin bounding brown clay layers; poly as fine needles or tiny plates on halite boundaries in fine-medium opaque halite	
Run #30	39.0	100%	85%		halite, medium-coarse, clear; non-halite components estimated <0.1%	
1340	39.90					
	40.0					

Attachment 1 – Core Log

Hole ID: SDI-BH00004	CORE LOG (cont. sheet)	Sheet _11_ of _13_
Logged by: Wayne Stensrud		Date: 1/7/14

Run Number	Depth (ft)	% Recovered	RQD	Profile (Rock Type)	Description	Remarks
	40.0				(29.90'–50.6') Halite	H-1 (cont.)
Run #31	41.0	100%	75%		halite, as above; trace polyhalite & clay	
	41.30					
Run #32	42.0 42.65	100%	81%		halite, medium-coarse, no poly or clay	
Run #33	43.0 44.0	100%	93%		halite, coarse-very coarse; no polyhalite, trace clay(?)	

1/7/14

14.05

14:14

Attachment 1 – Core Log

		CORE LOG (cont. sheet)		Sheet 12 of 13
Hole ID: SDI-BH00004				
Logged by: Wayne Stensrud			Date: 1/7/14	

1/7/14
1425

Run Number	Depth (feet)	% Recovered	RQD	Profile (Rock Type)	Description	Remarks
	44.0				(29.90'-50.6') Halite	H-1 (cont.)
Run #34		100%	96%			
	45.0					
	45.30					
Run #35		100%	82%		halite, coarse-very coarse, generally clear to light orange (lower 0.3'); no clay; trace anhydrite as thin, discontinuous stringers	
	46.0					
	46.65				halite, clear to orange, fine-coarse, with thin, discontinuous polyhalitic bands and some broader distribution; poly <1% average	
Run #36	47.0	100%	100%			
	47.93					
	48.0					

1438

1442
1/8/14 0800

Attachment 1 – Core Log

Y8/14

Hole ID: SDI-BH00004	CORE LOG (cont. sheet)	Sheet 13 of 13
Logged by: Wayne Stensrud		Date: 1/8/14

Run Number	Depth (ft)	% Recovered	RQD	Profile (Rock Type)	Description	Remarks
	48.00					
Run #37	49.00	100%	96%		(29.90'-50.6') Halite halite, fine-very coarse; coarse is clear, fine-medium is gray, very fine-fine is orange; <1% non-halite overall; polyhalite is in discontinuous zones <1/2" thick and as one poorly defined pod; poorly defined sub-horizontal gray zones have anhydrite and possibly trace clay.	H-1 (cont.)
0830	49.30					
Run #38	50.0	100%	100%			
0850	50.60				Total Depth=50.6'	
	51.00					
	52.00					

Attachment 1 – Core Log

CORE LOG		Sheet _1_ of _13_

Hole ID: SDI- BH00005   Location: N 780 E 1310

Drill Date: 1/8/14 – 1/10/14
Drill Crew: Blas, Heime, Wes, Troy

Drill Method: Reverse Rotary
Hole Diameter: 4- 5/8"
Hole Depth: 50. 8 ft
Hole Orient: Vertical UP

Drill Make/Model: Atlas Copco Drinet 264
Barrel Specs: 4⅝ OD x 3¾ ID x 15"
Drill Fluid: AIR
Core Preserv: Cellophane and Heat Seal

Logged by: Wayne Stensrud   Date: 1/8/14 – 1/10/14   Scale: ____

Survey Coordinates: (Ft)	Northing	Easting	Elevation
	10 475. 38	8210.83	1304. 85

Comments: Cored described by Wayne Stensrud, Core marked and preserved by Brian Dozier, and David Grvein Los Alamos National Laboratories.

Time	Run Number	Depth (ft)	% Recovered	RQD	Profile (Rock Type)	Description	Remarks

Time							
1030		0.0				0-4.65 Halite Clear to moderate reddish orange/brown. Coarse Crystalline, Some fine to medium locally. <1% Polyhalite and gray Clay.	Mu-6
	Run #1	1.0	100%				Confirm <1% poly; no discernible clay; poly in stringers and some blebs
1042		1.30					
12:24	Run #2	2.0	0%	0	Lost Core		
12:43		2.60					
	Run #3	3.0	100%	46%			
1250		3.90					
1258							

(Continue data on following page[s], as necessary.)

Information Only

Attachment 1 – Core Log

Vertical Up Hole (handwritten, left margin)

		CORE LOG (cont. sheet)		
Hole ID: **SDI-BH00005**			Sheet **2** of **13**	
Logged by: **Wayne Stensrud**		Date: **1/8/14 – 1/10/14**		

Run Number	Depth (ft)	% Recovered	RQD	Profile (Rock Type)	Description	Remarks
Time	4.0					
Run #4		100 %	100%	x — / — x / — —	From 4' up, </1/2% gray clay as short stringers in very coarse, very clear halite; some clasts (?) of very fine orange halite in coarse halite; poly less than below.	MU-6 (Cont)
	5.0			x	4.65-7.0 Halite Clear to Light medium gray Some reddish orange. Coarsely Crystalline. Some fine to medium Locally. Less than ½ % gray clay and poly halite.	MU-7
1301	5.15					
1310						
Run #5		100 %	1.4/1.4 = 100%	x / — / —		
	60			x / —		
1318	6.55			— x	Halite, gray to orange, fine-coarse; ~1% clay, <1/2% poly; clay generally distributed between halite crystals; thin gray clay under anhydrite b.	
1323		88%		— / x / —		
Run #6	7.0			[hatched] LostCore x	7.0-7.2 Anhydrite b Light to medium gray. Microcrystalline Anhydrite Some halitic growths. Thin gray clay seam at base of unit.	MU-8
			69%			
1334	7.85			x	7.3-11.9 Halite	MU-9
1341	8.0					

Attachment 1 – Core Log

Vertical
up
Hole

		CORE LOG (cont. sheet)		
Hole ID: SDI-BH00005			Sheet 3 of 13	
Logged by: Wayne Stensrud		Date: 4/8/14		

Time	Run Number	Depth (ft)	% Recovered	RQD	Profile (Rock Type)	Description	Remarks
		8.0					
4/8/14	Run #7		~75%	0% 0	No Core X	(7.3'-11.9') Halite clear to Light reddish orange, coarsely crystalline some medium. Scattered Anhydrite Stringers. Contact with unit below is sharp. None to < ½% polyhalite. Trace of Gray Tray Locally.	MU-9
		9.0			X		
1348		9.15					
1354	Run #8		~75%	0%	X No Core		
1400		9.95			HH		
1410	Run #9		~70%	0%	Lost Core		
1438		10.6					
	Run #10	11.0	100%	31%		Halite, clear, medium-coarse, with thin gray clay or anhydrite draping halite crystals along subhorizontal direction.	
1/9/14		11.9					MU-10

Attachment 1 – Core Log

Vertical
up
Hole

1/9/14
Time

	CORE LOG (cont. sheet)	
Hole ID: SDI-BH-00005		Sheet 4 of 13
Logged by: Wayne Stensrud	Date: 1/9/14	

Run Number	Depth (ft)	% Recovered	RQD	Profile (Rock Type)	Description	Remarks
	12.0					
Run #11		100%	43%	x x x	(11.90'-12.95') Halite and Brown Clear to reddish orange, fine to coarsely crystalline. 10% Brown clay or gray clay and dispersed polyhalite. Contact with lower unit is difused based on crystal size and amounts of clay and polyhalite → Clay H at Base	MU-10 (cont) Fine halite dominates above 12.0 ft; efflorescent salt
Run #12	12.95 14.0	88%	33%		(12.95'-13.60') Anhydrite 'a'. Light to medium gray, light brownish gray. Microcrystalline. Halitic Zone < 1" Thick. Halitic Swallowtail growths. Coarsely crystalline. Thin gray clay 'H' at Base.	Mu-11 Mu-12
Run #13	14.15 15.0 15.35	100%	0%	x x x x x	(13.60'-17.80') Polyhalitic Halite Clear to moderate reddish-orange, coarsely crystalline. 1 to 3% polyhalitic and polyhalitic Blebs. Contact with unit below is sharp.	
Run #14	16.0		0%	x x x		

0747
0807
0815
0825
0848

Attachment 1 – Core Log

	CORE LOG (cont. sheet)		
Hole ID: SDI-BH00005		Sheet 5 of 13	
Logged by: Wayne Stensrud		Date: 1/9/14	

1/9/14 Time	Run Number	Depth (ft)	% Recovered	RQD	Profile (Rock Type)	Description	Remarks
		16.0					
	Run #14		100%	0%	X X X	(13.60-18.7') Polyhalite Halite	Mu-12 (Cont.)
0854		16.75					
0906		17.0			X		
	Run #15		100%	37%	X X X		
0909		18.0					
0920		18.10					
	Run #16		100%	74%	X	(18.7'-20.58') Halite. Clear to moderate reddish-orange, moderate Brown to gray. medium to coarsely crystalline, some fine. 1% Brown Clay. Trace of gray Clay. <1% dispersed poly halite. Contact with unit below is gradational based on Clay and polyhalite Content.	Mu-13 Halite becomes finer upward from 18.3 ft; poly and anhydrite disseminated and some stringers; very little clay; 1/2-1% sulfate
0928		19.0					
0938	Run #17	19.45	100%				
		20.0					

Information Only

Attachment 1 – Core Log

		CORE LOG (cont. sheet)		
Hole ID: SDI-BH00005				Sheet 6 of 13
Logged by: Wayne Stensrud		Date: 1/9/14		

1/9/14 Time	Run Number	Depth (ft)	% Recovered	RQD	Profile (Rock Type)	Description	Remarks
	Run #17	20.0	100%	75%		(18.7' – 20.58') Halite	MU-13 (cont.)
0953	Run #18	20.58 / 21.0 / 21.31	88%	70%		(20.58' – 21.45') Halite Clear to gray Coarsely Crystalline, Scattered Discontinuous Anhydrite stringers. Dispersed polyhalite	MU-14
	Run #19	22.0 / 22.61	100%	85%		(21.45' – 22.9') Halite Clear to orange to Brown some gray, medium to Coarsely Crystalline. Some fine. Dispersed poly halite 1% Brow clay up to 3% Locally. Argillaceous Halite Locally	clay is in zones or intervals, between crystals; polyhalite <1%, localized between halite.
1020		23.0		0%			clay is localized in desiccation crack
11:45	Run #20	23.97	100%			(22.9' – 27.65') Halite Clear, Coarsely Crystalline up to 1% poly halite and Brown Clay. Scattered Anhydrite. 1% Brown Clay	MU-15

Description area annotations (red):
Halite, coarse, clear, with local 5% clay →
← fine polyhalite in halite

Attachment 1 – Core Log

	CORE LOG (cont. sheet)		
Hole ID: SDI-BH-00005		Sheet 7 of 13	
Logged by: Wayne Stensrud		Date: 1/9/14	

Time	Run Number	Depth (ft.)	% Recovered	RQD	Profile (Rock Type)	Description	Remarks
1/9/14		24.0					
	Run #21	25.0	100%	0%		(22.9'- 27.65') Halite	Mu-15 (cont.)
1240		25.25					
	Run #22	26.0	82%	0%			
1245		26.65					Halite
	Run #23	27.0	100%	88%			
1300		27.90				(27.65'- 28.85') Argillaceous Halite. Moderate brown fine grain to medium crystalline.	AH-1
1312		28.0					

Attachment 1 – Core Log

| Hole ID: SDI-BH00005 | CORE LOG (cont. sheet) | Sheet 8 of 13 |
| Logged by: Wayne Stensrud | | Date: 1/9/14 |

Run Number	Depth (ft)	% Recovered	RQD	Profile (Rock Type)	Description	Remarks
	28.0					
Run #24		93%	93%		brown clay is 1-3%, distributed in different zones; from exposure/desiccating depositional zone; no clay 29.0 ft.; contact at 28.8 ft gradational over ~1/2 inch.	A H-1 (cont)
	29.0				28.85 - 30.60 Halite Clear to Light Brown. Coarsely Crystalline. Contact with Clay J below is gradational. < 1/2% Brown Clay.	H-5
	29.30					
1327						
Run #25		100%				
	30.0					
			31%			
1332						
1341	30.60				30.60 - 35.60 Argillaceous Halite moderate Brown, some reddish orange. Coarse Crystalline some medium, some fine Locally. 1 to 3% Brown Clay, some gray. < 1/2% dispersed polyhalite. Contact with Lower unit is gradational based on Clay Content. Discontinuous Partings	AH-2 clay is localized
Run #26	31.0					
		100%	44%			
	31.95					
13:57	32.0					

Information Only

Attachment 1 – Core Log

	CORE LOG (cont. sheet)	
Hole ID: SDI-BH-00005		Sheet 9 of 13
Logged by: Wayne Stensrud	Date: 1/9/14	

Time	Run Number	Depth (ft)	% Recovered	RQD	Profile (Rock Type)	Description	Remarks
1/9/14 1354	Run #27	32.0	100%	100%		Argillaceous Halite (cont)	AH-2 (cont)
1401 1410		33.0 33.20					
	Run #28	34.0	100%	100%		as above shows discontinuous brown clay stringers, horizontal to curved and subhorizontal	
	Run #29	34.65 35.0	100%	69%		fine halite increases upward to well defined clay K	
						Clay 'K' ~½" Thick	
		35.95 36.0				35.60-36.80 Anhydrite. Light to medium gray, microcrystalline,	MB138

Attachment 1 – Core Log

Hole ID: SDI-BH00005	CORE LOG (cont. sheet)	Sheet _10_ of _13_
Logged by: Wayne Stensrud		Date: _1/9/14_

Time	Run Number	Depth (ft)	% Recovered	RQD	Profile (Rock Type)	Description	Remarks
1/9/14 Time		36.0					
	Run # 30		100%	63%		Anhydrite. Lower portion laminated. Upper portion scattered halitic growths. Clay Seam K at Base of Unit ~ ½" Thick. Contact with unit Below is Sharp at K	MB 138 (cont)
		37.0				36.80 - 39.50 Halite	H-6
1/10/14 0800		37.30				Clear to moderate reddish-orange. Coarsely Crystalline to medium. 1 to 3% Polyhalite. Anhydrite Stringers. Scattered Brown Clay Locally. Contact with MB 138 Below is Sharp.	→ and Brown
	Run # 31	38.0	100%	0%			
						verified	
0816		38.64					
	Run # 32	39.0	100%	0%			
						39.50'-44.7' Halite	H-7
						very low clay at contact	
0920		40.0					

Attachment 1 – Core Log

CORE LOG (cont. sheet)			
Hole ID: SDI-BH00005			Sheet 11 of 13
Logged by: Wayne Stensrud		Date: 1/10/14	

Time 1/10/14	Run Number	Depth (ft)	% Recovered	RQD	Profile (Rock Type)	Description	Remarks
		40.0					
0836	Run # 33		100 %	29 %		(39.50'- 44.70') Halite, clear to reddish orange to moderate brown coarsely crystalline, some fine to medium. < 1% Brown and grey clay. Scattered breaks. Locally Argillaceous. Contact with below is gradational based on Clay and polyhalitic Content < 1% Polyhalite. Clay Stringers.	H-7 (cont)
		41.0					clay content up to ~46.8 ft is estimated to average ~3%; distributed in subhorizontal clay stringers
0838		41.40					
0854	Run # 34	42.0	100%	65 %			
0855		42.70					
0910		43.0					
0913	Run # 35	44.0	100%	0%			

Attachment 1 – Core Log

| Hole ID: SDI-BH00005 | | CORE LOG (cont. sheet) | Sheet 12 of 13 |
| Logged by: Wayne Stenswd | | Date: 1/10/14 | |

	Run Number	Depth (ft)	% Recovered	RQD	Profile (Rock Type)	Description	Remarks
1/10/14		44.0					
0925	Run #36		100%	60%		Halite (cont)	H-7 (cont)
		45.0				clay seam	verified
0930		45.4				(44.7'-46.85') Argillaceous Halite. Clear to reddish-orange to Brown. Coarsely Crystalline, Some fine to medium. <1 to 5% Brown clay some gray. Locally up to 10% Clay. Intercrystalline scattered Breaks. Contact with Lower unit is gradational based on Clay Content.	AH-3
0943	Run #37	46.0	100%	100%			
						clay seam	verified, strongly developed clay stringers
0949		46.70				clay seam	
1002	Run #38	47.0	100%			(46.70'-50.8') Polyhalitic Halite. Clear to moderate reddish orange and Brown. Coarsely Crystalline, Some medium. <1 to 3% polyhalite. None to 1% brown Clay and Some gray Clay.	PH-5 poly is blebs and halite crystal films; clay is disseminated blebs to absent, found in zones with non-argillaceous halite between
		48.0					

Attachment 1 – Core Log

| Hole ID: SDI-BH00005 | CORE LOG (cont. sheet) | Sheet 13 of 13 |
| Logged by: Wayne Stensrud | Date: 1/10/14 | |

Run Number	Depth (ft.)	% Recovered	RQD	Profile (Rock Type)	Description	Remarks
	48.0					
1006 Run #39	48.15	100%	32%	x x x — x x — x	Poly halitic Halite	PH-5 (Cont)
	49.0					
1024 1038 Run #40	49.4 50.0	100%	0%	x — x — x x — x — x x — x x — x x —		local irregular limited anhydrite
1043	50.8 51.0			x —	Bottom of Hole 50.8'	
	52.0					